Solar Energy 212 (2020) 203–219

Contents lists available at ScienceDirect

Solar Energy

journal homepage: www.elsevier.com/locate/solener

Control algorithms applied to active solar tracking systems: A review

Rosa F. Fuentes-Morales [a], Arturo Diaz-Ponce [b,*], Manuel I. Peña-Cruz [b], Pedro M. Rodrigo [d,e], Luis M. Valentín-Coronado [b], Fernando Martell-Chavez [c], Carlos A. Pineda-Arellano [b]

[a] PICYT - Centro de Investigaciones en Óptica, A.C. Unidad Aguascalientes, Prol. Constitución 607, Fracc. Reserva Loma Bonita, Aguascalientes, Aguascalientes 20200, Mexico
[b] CONACYT – Centro de Investigaciones en Óptica, A.C. Unidad Aguascalientes, Prol. Constitución 607, Fracc. Reserva Loma Bonita, Aguascalientes, Aguascalientes 20200, Mexico
[c] Centro de Investigaciones en Óptica, A.C. Unidad Aguascalientes, Prol. Constitución 607, Fracc. Reserva Loma Bonita, Aguascalientes, Aguascalientes 20200, Mexico
[d] Centre for Advanced Studies in Energy and Environment (CEAEMA), University of Jaén, Jaén 23071, Spain
[e] Universidad Panamericana, Facultad de Ingeniería, Josemaría Escrivá de Balaguer 101, Aguascalientes, Aguascalientes 20290, Mexico

ARTICLE INFO

Keywords:
Solar tracking
Control algorithm
Open-loop
Closed-loop
Hybrid-loop

ABSTRACT

It is well known that concentrating solar power and concentrating photovoltaic technologies require high accuracy and high precision solar tracking systems in order to achieve greater energy conversion efficiency. The required tracking precision depends primarily on the acceptance angle of the system, which is generally tenths of a degree. Control algorithms applied to active solar tracking systems command and manipulate the electrical signals to the actuators, usually electric motors, with the goal of achieving accurate and precise solar tracking. In addition, a solar tracking algorithms system must provide robustness against disturbances, and it should operate with minimum energy consumption.

In this work, a systematic review of the control algorithms implemented in active solar tracking systems is presented. These algorithms are classified according to three solar tracking control strategies: open-loop, closed-loop and combined open- and closed-loop schemes herein called hybrid-loop. Their working principles as well as the main advantages and disadvantages of each strategy are analyzed. It is concluded that the most widely used solar tracking control strategy is closed-loop, representing 54.39% of all the publications consulted. On–off, fuzzy logic, proportional-integral-derivative and proportional-integral are the control algorithms most applied in active solar tracking systems, representing 57.02%, 10.53%, 6.14% and 4.39%, respectively.

1. Introduction

Over the past few years, solar energy harvesting systems have presented great technological advances (Murdock et al., 2019). To take advantage of this solar resource, two technologies have mainly been exploited: photovoltaic (PV) and concentrating solar power (CSP) systems (Bosetti et al., 2012). PV systems are divided into two subgroups: conventional photovoltaic, which takes advantage of the directly received sunlight and converts it into electricity without the need for another optical element; and concentrating photovoltaic (CPV), which employs an optical element, typically a linear focus or point focus lens or mirror in order to concentrate sunlight on a small photovoltaic receiver (Khamooshi et al., 2014). Similarly, CSP technology uses optical elements to concentrate the sunlight on a small area, where a thermal receiver is placed. In addition to PV and CSP technologies, there are hybrid plants that incorporate both solar technologies. One of the greatest considerations for deploying CPV and CSP systems is that these technologies require active solar tracking systems (ASTS).

ASTS can be classified, depending on its degrees of freedom, into one-axis, two-axis or multiple-axis systems (Nsengiyumva et al., 2018; Prinsloo and Dobson, 2015; Alexandru, 2013; Singh et al., 2018). These systems can significantly increase the amount of produced energy, especially in the early morning and late afternoon when the angular relationship of the direct solar irradiance with surface is smaller (Camacho and Berenguel, 2012). The energy conversion efficiency of PV systems can be increased by 12% to 25% with one-axis solar tracking (ST) and 30% to 45% with two-axis ST (Singh et al., 2018). Different aspects focused on the methods and designs of ASTS have already been analyzed in several works. In the work of Khalil et al. (2017), a review of ST techniques in PV power plants is presented, and its advantages and disadvantages are evaluated, including drive methods, control units,

* Corresponding author.
E-mail address: adiaz@cio.mx (A. Diaz-Ponce).

https://doi.org/10.1016/j.solener.2020.10.071
Received 15 July 2020; Received in revised form 22 October 2020; Accepted 24 October 2020
Available online 22 November 2020

Nomenclature

Abbreviations

ANFIS	Adaptive neural fuzzy inference system
ASTS	Active solar tracking systems
CA	Control algorithm
CCD	Charged-coupled device
CPV	Concentrating photovoltaic
CSP	Concentrating solar power
FLC	Fuzzy logic control
FOV	Field of view
FPGA	Field-programmable gate array
GPS	Global positioning system
HCPV	High concentration photovoltaic
IMC	Internal model control
LDR	Light dependent resistor
LQR	Linear quadratic regulator
MCU	Microcontroller unit
MDOF-SUI PID	Multi-degree of freedom-simplified universal intelligent PID
PC	Computer
PI	Proportional-integral
PID	Proportional-integral-derivative
PLC	Programmable logic controller
PV	Photovoltaic
SMC	Sliding mode control
SPA	Solar position algorithm
ST	Solar tracking
STE	Solar tracking error

Latin Characters

$FOV_{SunSensor}$	Field of view Sun sensor [°]
I_{sc}	Short-circuit current [A]
P_m	Maximum power [W]
$P_{Tracker}$	Position of the solar tracker [°]
SP_{Sensor}	Sun's position measured by the solar sensor[°]
SP_{SPA}	Sun's apparent position [°]
$STE_{ClosedLoop}$	Closed-loop solar tracking error [°]
$STE_{OpenLoop}$	Open-loop solar tracking error [°]
V_{oc}	Open-circuit voltage [V]

types of tracking and the percentage of gained energy in comparison with fixed PV systems. In another review of ST methods and maximum power point tracking (MPPT) algorithms, Sumathi et al. (2017) concluded that the increase in average energy production in several PV systems with a two-axis ST was approximately 30% with respect to the fixed system. Comparably, Motahhir et al. (2020) presented a detailed review of MPPT algorithms where their principles of operation and main characteristics were studied. The authors analyzed the suitability of several low-cost embedded systems for each MPPT algorithm based on its complexity and structure. Similarly, the reviews presented by Hafez et al. (2018), Mousazadeh et al. (2009), Awasthi et al. (2020), Nsengiyumva et al. (2018) and Nadia et al. (2018) classified the ASTS in different categories based on their ST technologies. Furthermore, their advantages and disadvantages were discussed, and their applications were mentioned. Finally, Lee et al. (2009) described some proposals for open- and closed-loop types of ASTS developed over the past 20 years. It is worth mentioning that the works mentioned above do not focus on the control algorithm (CA) used to command the electrical signals to the actuators of the ASTS.

On the other hand, a summary of methodologies available for characterizing the solar tracking error (STE) of five parabolics through collectors is presented in Sallaberry et al. (2017). The authors employ different methodologies to measure the STE, and they analyzed the optical losses of each system. Standardized instrumentation capable of providing enough sensitivity to gauge sub-degree accuracy ranges does not exist, however, at the present stage (IEC et al., 2014). Therefore, all the studies either follow different STE measurement techniques or do not present a tracking error at all (Luque-Heredia et al., 2012; Cristobal et al., 2012). Recently, the International Electrotechnical Commission (IEC) has created the IEC 62817 standard, which is an international design qualification standard that defines test procedures under a standardized methodology for solar tracking systems (IEC et al., 2014). Sallaberry et al. (2015) presented an interesting study with the characterization of a one-axis solar tracker. In this work, a testing procedure adapted from the IEC 62817:2014 standard for ones-axis solar trackers was defined. Similarly, in evaluations of this standard, Aipperspach et al. (2015) and Casajús and Muñoz (2016) identified some difficulties, and they proposed improvements to consider for the next update of the standard.

As observed in the aforementioned papers, there are several works reviewing ASTS. Most of them, however, focus on the classification of different types of ST systems, their pros and cons, design methodologies and their implementation in different solar energy harvesting systems. The work presented here summarizes the CAs applied to ASTS, both simulated and experimental, with the aim of knowing the STEs reported and the most widely used algorithms, solar sensors, control units and Sun localization methods. In this paper, Section 2 describes the generalities of ASTS applied to CSP, PV and CPV systems. In addition, the impact of the STE on two high concentration photovoltaics (HCPV) modules is analyzed. Section 3 presents an analysis of the operating principle and pros and cons of solar tracking strategies: open-loop, closed-loop and hybrid-loop, and the control algorithms applied in each strategy. In Section 4, an alternative classification of control algorithms applied to ASTS taking into account their control unit is presented. Finally, the discussion and conclusions are presented in Sections 5 and 6, respectively.

2. Active solar tracking systems (ASTS)

ASTS are mechanisms capable of changing the position of solar power systems to increase the uptake of energy by orienting the systems perpendicularly to solar rays. Typically, the ASTS include several components, such as transmission mechanical drive subsystems, electric motors, sun position sensors, solar position algorithms, control units and limit switches (Prinsloo and Dobson, 2015). The objectives of the ASTS are to achieve high precision ST, robustness against disturbances, high stability, soft control signals and ease of implementation. Furthermore, the energy consumption of the solar tracker should be 2% to 3% of the increased energy in a solar power generation system (Mousazadeh et al., 2009). Sefa et al. (2009) presented the comparison of the main construction parameters of ASTS. One of the main differences is the ST precision, which increases the conversion efficiency of solar energy into thermal or electrical energy (Rubio et al., 2007). Commonly, the minimum ST precision required is established by means of the acceptance angle of the concentration system, usually defined as the off-tracking angle at which power generation decreases below 90% (Luque-Heredia et al., 2012). The more accurate the solar tracking, the greater the efficiency of the solar power generation systems (Sallaberry et al., 2017; Lee et al., 2009; Camacho and Berenguel, 2012; Perers et al., 2013; Awasthi et al., 2020).

The performance reduction factors of the systems that harness solar energy were classified into two main types: (1) factors related to the ST precision and (2) factors that account for or consider a reduction of the acceptance angle of the systems (Luque-Heredia et al., 2012). In the

same way, the factors conditioning ST precision can be classified according to their nature as shown in Table 1. On the one hand, the software-defined component includes all the problems where the software is the focus and is used to provide the solution, such as the control algorithms, SPA, ST frequency, among others. This component can be quickly addressed without the need for mechanical modifications. On the other hand, the hardware-defined component refers to the physical parts that require major changes in order to improve the performance of ASTS, for instance, electronic devices, sensors, actuators, unit control, and so forth. The cheapest and sometimes simplest way to increase the precision and accuracy of ASTS is to optimize the control software. A simple change in the CA can significantly improve the ST performance. For example, Garrido and Díaz (2016) presented a performance study of a one-axis ST prototype controlled by two different closed-loop CAs. The achieved ST precision was different in both algorithms. Similarly, Fathabadi (2016a) presented a comparison of two ST strategies in the same ST mechanism: open-loop and closed-loop. The results concluded that the closed-loop ST strategy obtained more energy production in a PV module with respect to the open-loop.

As previously mentioned, the acceptance angle of the CSP and CPV systems define the tolerance of ST accuracy. This angle varies according to the construction characteristics of each system and is generally tenths of a degree. In the case of conventional PV systems, the ST precision is not a crucial factor because its acceptance angle is very large in relation to the acceptance angle of CSP and CPV systems. The following subsection experimentally analyzes the sensitivity of the electrical response of two point-focus Fresnel lens-based CPV modules relative to the STE.

2.1. Impact of solar tracking error in CPV modules

In CPV systems, a large quantity area of optical elements is used to concentrate the sunlight onto small-sized multi-junction PV cells. The typical commercial CPV modules consist of a Fresnel lens array. Each Fresnel lens focuses light on a single solar cell (point-focus), which is electrically interconnected in series to achieve a two-terminal module. Highly precise two-axis solar tracers are required to keep the CPV modules perpendicular to solar rays. In HCPV modules, the concentration levels commercially available are between 500*x* and 1300*x*, and the acceptance angles of the modules are quite small (with half acceptance angle between 0.7° and 1.9°) (Pérez-Higueras et al., 2018a; Pérez-Higueras and Fernández, 2015). High efficiency is one of the key motivations for developing more cost-competitive HCPV systems, in agreement with the levelized cost of energy (LCOE) (Kost et al., 2013; Wiesenfarth et al., 2017). The sensitivity of the electrical response of a CPV module relative to the STE can be measured with special solar simulators, such as the Helios 3198 shown in Fig. 1 (Domínguez et al., 2008). To perform a test, the CPV modules are mounted on an adjustable support structure. By controlling the position of the structure, the modules can be measured at different tilt angles relative to the direction of the collimated light. Therefore, the electrical response of the modules for different STEs can be obtained. An electronic load synchronized with the Xenon lamp registers the electrical measurements.

An illustration of how the acceptance angle can be measured with the solar simulator is depicted in Figs. 2 and 3 by measurements performed on two CPV modules of different manufacturers, module A and B. Although the whole current–voltage (I-V) curve is measured, the graphs summarize the most important electrical parameters of the CPV module: open-circuit voltage (V_{oc}), short-circuit current (I_{sc}), and maximum power (P_m). As exhibited, the tracking error mainly influences the I_{sc}, keeping the V_{oc} almost constant. The P_m decreases faster than the I_{sc} because of the degradation of the I-V fill factor as the tracking error increases. The CPV module A reaches 90% of the initial I_{sc} for a tracking error of 0.69°, while the CPV module B reaches 90% of the initial I_{sc} for a tracking error of 0.90°. Thus, the CPV module B shows a better angular response. These kinds of graphs illustrate the critical impact of the STEs on the electricity generation of CPV systems (Victoria et al., 2009).

Table 1
Factors conditioning solar tracking precision in ASTS.

Software-defined component
· ST strategy (Open-, closed- or hybrid-loop) (Luque-Heredia et al., 2004; Safan et al., 2017).
· Control algorithm (On–off, PI, PID, etc) (Luque-Heredia et al., 2004; Safan et al., 2017).
· ST frequency (Mi et al., 2016).
· Solar position algorithm (SPA) (Luque-Heredia et al., 2012).
· Geographic positioning deviation in the SPA (Rubio et al., 2007).
Hardware-defined component
· Types of ASTS.
· Actuator type and gear ratio.
· Unit control type (Luque-Heredia et al., 2012).
· Backlash of the actuators (Fernandez-Prieto et al., 2020).
· Characteristics of the solar sensor (Luque-Heredia et al., 2012).
· Mismatch of photosensors.
· Installation deviation (Burhan et al., 2016; Fernandez-Prieto et al., 2020; Luque-Heredia et al., 2012).
· Lack of maintenance (Luque-Heredia et al., 2012; Nsengiyumva et al., 2018).
· Lack of calibration in sensors (Fernandez-Prieto et al., 2020).
· Errors due to wind effects (Zhang et al., 2019; Fernandez-Prieto et al., 2020; Luque-Heredia et al., 2012).

3. Classification of control algorithms applied to ASTS

In order to analyze the different solar tracking strategies and the CAs applied to ASTS, this section presents a classification of the works related to ASTS found in the literature. This classification was made according to the ST strategy: open-loop, closed-loop or hybrid-loop, as can be seen in Table 2. This table shows that the classic control algorithms: on–off, PI and PID were implemented by 67.55% of the works found in the literature, and the on–off control is the most used CA. In addition, from research studies analyzed, 28.95% implemented an open-loop strategy, 54.39% apply a closed-loop, and only 16.67% used a hybrid-loop strategy. It is worth noting that only studies in which CAs are presented or in which the algorithms can be directly determined, were considered. The results or main findings of the reviewed works were obtained directly from what was reported. It is necessary, however, to remark that they were not characterized under the same testing/simulation conditions, and, therefore, a universal evaluation criterion cannot be established.

The following subsections detail the ST strategies, and their main advantages and disadvantages, operating principle and control diagram

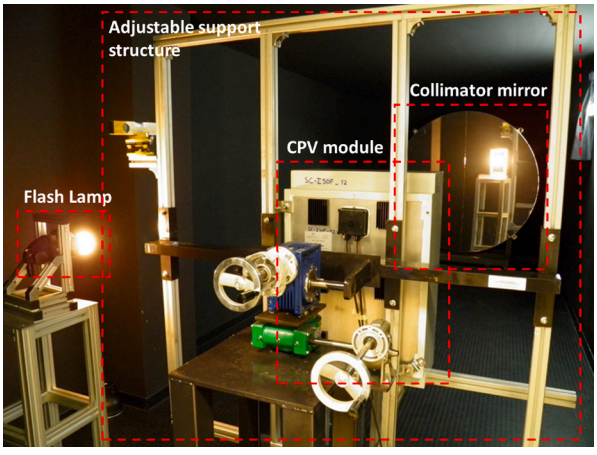

Fig. 1. Helios 3198 CPV solar simulator (figure taken from Pérez-Higueras et al. (2018b)).

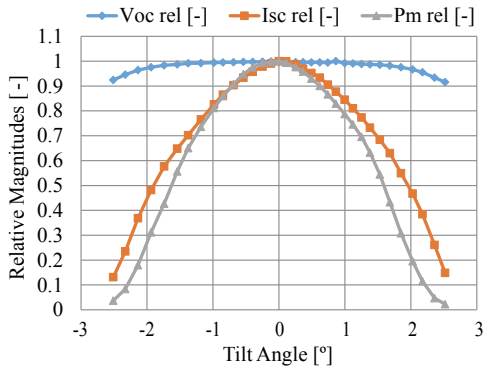

Fig. 2. Acceptance angle at 1000 W/m^2 in the CPV module A measured in the solar simulator.

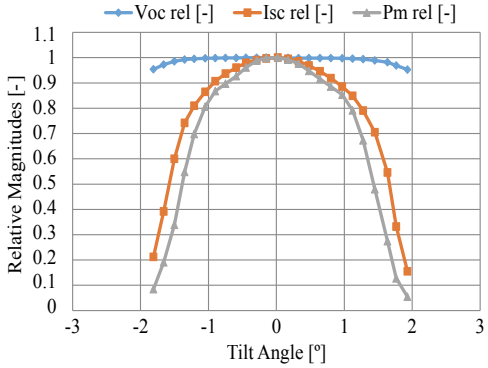

Fig. 3. Acceptance angle at 1000 W/m^2 in the CPV module B measured in the solar simulator.

are described. In addition, in order to differentiate the studies considered in this review, some of the most important characteristics in ASTS are analyzed: control algorithm, tracking accuracy, tracker type, motor type, solar localization method and unit control. It should be pointed out that most of the studies found in the literature do not apply the IEC 62817 standard. Therefore, it is not feasible to perform an objective comparison.

3.1. Open-loop solar tracking strategy

This ST strategy is called open-loop because there is no control feedback from a solar sensor. As can be seen in the block diagram shown in Fig. 4, this strategy employs an SPA based on the solar coordinates to estimate the Sun's apparent position with respect to a geographical location on Earth. This algorithm is usually programmed in a electronic control unit such as a computer (PC), Arduino, microcontroller (μC) or in a programmable logic controller (PLC). Once the SPA calculates the solar zenith and azimuth angles, it is necessary to transform them in the control unit into angular position for the actuators of the ASTS. Finally, the rotation angles are commanded through a control signal (u) towards the tracker in order to automatically align the CSP or CPV system to the solar vector. This strategy is commonly implemented in low precision ASTS, and some of its advantages and disadvantages are shown in Table 3.

In the open-loop ST strategy, the SPAs require knowing parameters such as the geographic location, time, date, as well as the orientation of the ASTS (Blanco-Muriel et al., 2001; Reda and Andreas, 2004; Chong et al., 2009; Chong and Wong, 2010; Zhu et al., 2020; Debbache et al., 2016). The azimuth and zenith angles generated by the SPA represent the set point of the open-loop control as seen in Fig. 4. In this method, the error introduced by the use of photosensors in closed-loop systems

Table 2
Control algorithms for open-loop, closed-loop and hybrid-loop ST strategies applied to ASTS.

Control algorithm	Open-loop (28.95%)	Closed-loop (54.39%)	Hybrid-loop (16.67%)	Total average (100%)
Classic control (67.55%)				
On–off	57.58%	59.68%	47.37%	57.02%
Proportional-integral-derivative	6.06%	3.23%	15.79%	6.14%
Proportional-integral	3.03%	3.23%	10.53%	4.39%
Modern Control (32.45%)				
Fuzzy logic	6.06%	14.52%	5.26%	10.53%
Sliding mode	9.09%	1.61%	-	3.51%
PID-FLC	3.03%	3.23%	-	2.63%
Adaptive	3.03%	-	5.26%	1.75%
Neural network	-	3.23%	-	1.75%
Adaptive SMC	-	1.61%	-	0.88%
IMC-PID	-	1.61%	-	0.88%
Neuro-fuzzy logic	-	1.61%	-	0.88%
Cascade	-	1.61%	-	0.88%
Predictive	3.03%	-	-	0.88%
Parametric optimization	3.03%	-	-	0.88%
Distributed	-	-	5.26%	0.88%
Linear quadratic regulator	-	1.61%	-	0.88%
Machine learning	-	1.61%	-	0.88%
Kinematic synthesis	3.03%	-	-	0.88%
ANFIS	3.03%	-	-	0.88%
Robust control	-	1.61%	-	0.88%
Bayesian network	-	-	5.26%	0.88%
Logic-based supervisor	-	-	5.26%	0.88%

can be avoided since their operation is independent of weather conditions. Although an open-loop controller operates with a very precise SPA, it is affected, however, in the field by a set of error sources that can highly degrade its final tracking accuracy (Luque-Heredia et al., 2012):

- SPA inaccuracies or in the input parameters
- Tolerance of the manufacturing, assembly and installation processes of ASTS
- Errors or assumptions made in the process of transforming the solar coordinates into angles of rotation of the actuators
- Gravitational bending in wide aperture trackers
- Mechanical system resolution of the ASTS

Fig. 5 shows a typical flow chart of an open-loop ST strategy. Firstly, to calculate the Sun's apparent position, it is necessary to manually enter the latitude, longitude, orientation of the ASTS, date and time. The aforementioned can be avoided by using a GPS sensor, a magnetometer and a real-time clock. Considering this, an SPA calculates the azimuthal and zenithal angles of the Sun's apparent position (SP_{SPA}). These angles represent the set point of the CA, which finally commands the desired position to the actuators of the ASTS (as in Fig. 4). As mentioned above, the open-loop ST systems do not employ a solar sensor, so it is not possible to provide control feedback with the Sun's position. Some authors used encoders, or the pulses sent to ST stepper motors, to measure the position of the tracker ($P_{Tracker}$) (Fathabadi, 2016a; Chong et al., 2009; Pişirir and Bingöl, 2016). In these works, it is possible to calculate the open-loop solar tracking error ($STE_{OpenLoop}$) by using Eq. (1), which facilitates the establishment of the ST frequency or the tracking hysteresis allowed to optimize the production and consumption of energy in ASTS (Mi et al., 2016):

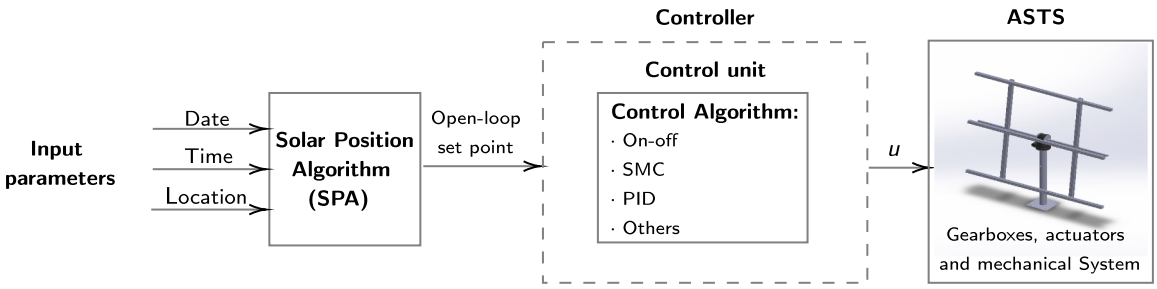

Fig. 4. Block diagram of a conventional open-loop ST strategy applied to ASTS.

Table 3
Advantages and disadvantages of the open-loop ST strategy in ASTS.

Advantages
· It does not require a solar sensor.
· Ease and low-cost of implementation.
· Operation is independent of weather disturbances.
Disadvantages
· Low tracking accuracy.
· It requires a SPA with the geographical data and time of solar tracking.
· It requires a sensor for the STE characterization.
· May require constant calibration.
· It can be unstable when faced with an electrical or mechanical disturbance.

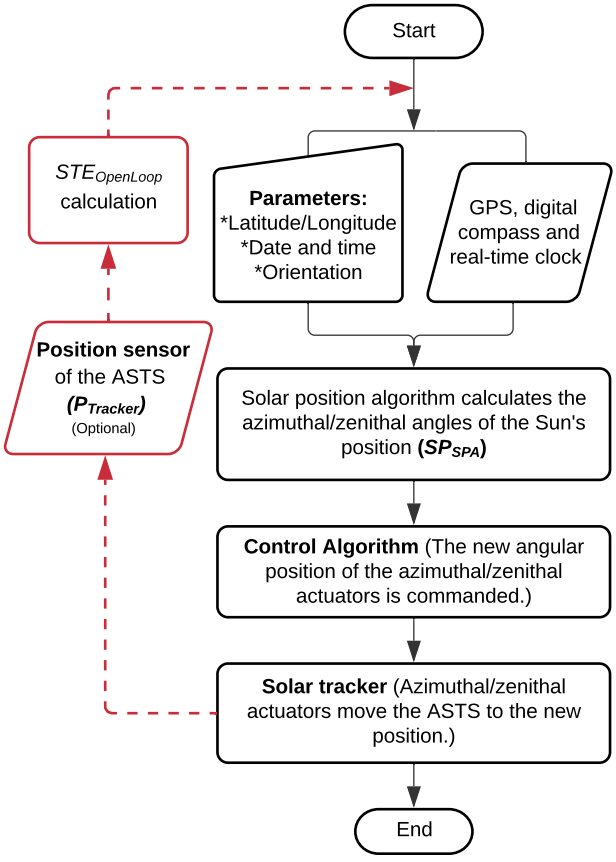

Fig. 5. Flow chart of an open-loop ST strategy for ASTS.

$$STE_{OpenLoop} = P_{Tracker} - SP_{SPA}. \quad (1)$$

The details of the studies that implement the open-loop ST strategy are presented in Table 2, of which 57.58% implement an on–off control, 9.09% a sliding mode control (SMC), 6.06% for proportional-integral-derivative (PID) and FLC, and 21.21% other types of controllers. It is important to emphasize that in this strategy the required control feedback of some algorithms is done using encoders or any position sensors as shown in Fig. 5; however, there is no solar sensor that directly measures and provides feedback about the Sun's apparent position. Table 4 details the found open-loop CAs. It can be observed that most are experimental works, and only some of them report the ST precision achieved. Note that each work uses different instruments and methodologies for measuring the STE, such as digital protractors by Fathabadi (2016b), a digital inclinometer by Sallaberry et al. (2015) or a CCD camera by Chong et al. (2009).

As can be seen in Table 2, the on–off CA is the most used algorithm in any of the three ST strategies because of its ease and low-cost implementation. This control is a discrete state algorithm that produces a continuous deviation from the set point value. Table 4 summarizes the open-loop ST works. Fathabadi (2016b) described an on–off CA in open-loop for a PV system with ST, which captured 24.59% more solar energy during one year with respect to a fixed PV system. The achieved STE was 0.43°. Similarly, 42.6%, 24%, 41.34% and 33% more energy was obtained in PV systems with ST controlled by on–off CAs compared with fixed PV in the works of Sungur (2009), Ruelas et al. (2019), Abdallah and Nijmeh (2004) and Rezoug and Chenni (2018), respectively. Sallaberry et al. (2015) proposed a procedure adapted from the IEC standard 62817 for the characterization of one-axis ASTS controlled with open-loop on–off algorithms. The optical losses were estimated by ray-tracing simulation, and the achieved STE was ±0.4°, which was experimentally measured by a digital inclinometer. Other interesting research presented an ST strategy with an on–off CA that is activated with different ST frequencies (Mi et al., 2016). This strategy was shown to save energy and improve the reliability of ASTS. Similar findings were found by Yang et al. (2017) and Elagib and Osman (2013), which used a GPS and a real-time clock module to determine the input parameters of an SPA programmed in a μC. The SPA estimates the Sun's position and establishes the open-loop set point of an on–off control for the tracker. The STEs are not mentioned. There are some studies that use on–off CAs that consider the optimal ST time interval in order to maximize the electrical energy production (Abdallah and Badran, 2008; Huang and Sun, 2007; Seme and Štumberger, 2011; Alexandru and Pozna, 2010). In these works, the efficient energy consumption of the ASTS is the most important feature, and the ST frequency is configured to achieve a good cost-benefit relationship.

SMC is the second most widely used CA in open-loop ASTS. This algorithm is a robust nonlinear control with discontinuous action, so it may be implemented by power converters with an on–off response. The CA coerces the system to slide along the boundaries of control structures. Although an SMC can produce extremely small errors, chattering in the control signal always exists. Accordingly, its implementation in ASTS is not very common since it requires high-frequency switching, which

Table 4
Summary of open-loop control algorithms applied to ASTS.

N	Authors	Exp./Sim.	Control algorithm	ST accuracy	Axis	Motor type	Sun localization	Control Unit
1	Sallaberry et al. (2015)	Exp.	On–off	±0.4°	One	-	SPA	-
2	Sungur (2009)	Sim.	On–off	-	Two	DC	SPA	PLC
3	Fathabadi (2016b)	Exp.	On–off	±0.43°	Two	Stepper	SPA	μC
4	Yang et al. (2017)	Exp.	On–off	-	Two	Stepper	SPA with GPS	μC
5	Allil et al. (2018)	Exp.	On–off	-	One	Stepper	SPA	μC Arduino
6	Mi et al. (2016)	Exp.	On–off	< 0.5°	Two	DC	SPA and optical sensors	-
7	Rezoug and Chenni (2018)	Exp.	On–off	-	Two	DC	SPA	μC
8	Ruelas et al. (2019)	Exp.	On–off	-	Two	DC	Tracking ranges	μC Arduino
9	Abdallah and Nijmeh (2004)	Exp.	On–off	-	Two	-	SPA	PLC
10	Skouri et al. (2016)	Exp.	On–off	< 0.2°	Two	DC	SPA	μC and PLC
11	Chong et al. (2009)	Exp.	On–off	0.17°	One	Stepper	SPA, CCD for monitoring	PC
12	Pişirir and Bingöl (2016)	Exp.	On–off	-	Two	Stepper	Software with database	PLC
13	Fathabadi (2016a)	Exp.	On–off	0.43°	Two	Stepper	SPA	μC
14	Abdallah and Badran (2008)	Sim.	On–off	-	One	-	Time intervals	PC
15	Huang and Sun (2007)	Exp.	On–off	-	One	-	Photosensor/Time intervals	PC
16	Seme and Štumberger (2011)	Sim.	On–off	-	Two	DC	SPA/Time intervals	PC
17	Alexandru and Pozna (2010)	Sim.	On–off	-	Two	DC	SPA/Time intervals	PC
18	Elagib and Osman (2013)	Exp.	On–off	0.1°	Two	DC	SPA with GPS	μC
19	Chowdhury et al. (2019)	Exp.	On–off	0.6°	Two	DC	SPA	μC
20	Rhif (2012)	Exp.	SMC	-	Two	Stepper	SPA	-
21	Rhif (2011)	Sim.	SMC	-	Two	DC	SPA	PC MATLAB
22	Keshtkar (2017)	Sim.	SMC	-	Two	three linear	SPA	-
23	Li et al. (2013)	Exp.	PI	-	Two	DC	SPA	μC
24	Sidek et al. (2017)	Exp.	PID	±0.5°	Two	DC	SPA with GPS	μC
25	Engin and Engin (2013)	Exp.	PID	0.1°	Two	DC	SPA with GPS	μC
26	Bedaouche et al. (2017)	Sim.	PID-FLC	-	Two	DC	SPA	PC Simulink
27	Fernandez-Prieto et al. (2020)	Exp.	FLC	-	Two	-	SPA	μC
28	Alata et al. (2005)	Sim.	FLC	-	One/two	-	SPA	PC MATLAB
29	Alexandru (2013)	Exp.	Parametric optimization	-	Two	DC	SPA	PC MATLAB
30	Ikhwan et al. (2018)	Sim.	Predictive model	0.027°/0.056°	Two	DC	SPA	PC Simulink
31	Ranganathan et al. (2011)	Sim.	Adaptive	-	One	-	SPA	dsPIC
32	Del Rosario et al. (2019)	Sim.	Kinematic synthesis	-	Two	-	SPA	PC MATLAB
33	AL-Rousan et al. (2020)	Sim.	ANFIS	-	One/two	-	SPA	PC MATLAB

could generate fatigue in the actuators and greater energy consumption. Rhif (2011) and Rhif (2012) presented, respectively, simulation and experimental results of the implementation of an SMC in an open-loop ST. The second one employed a sliding mode observer that replaces the velocity sensor. Experimental measurements show an increase in energy production by over 40% in a conventional PV system. Similarly, Keshtkar (2017) presented a simulation of a high order SMC that ensures finite-time convergence of the states to the desired trajectory, as well as the capacity of compensations of bounded perturbations in the ST. The authors concluded that SMC presented low sensitivity to external disturbances and uncertainties in the mathematical model of the ASTS.

There are several experimental studies that have implemented classic CAs in open-loop ASTS. Classical control tries to solve control problems for linear systems by a continuous response. Typically, in practice, these controllers are manually tuned by setting their parameters until obtaining a desired response. A prototype solar stove designed with a giant Fresnel lens with solar tracking through a PI control is presented by Li et al. (2013). In this system, the open-loop set point was established through an SPA, which uses a GPS for the input parameters. Because of the ST frequency of an on–off control, the defocus of the Fresnel lens was modeled and experimentally evaluated. In the works of Sidek et al. (2017) and Engin and Engin (2013), PID CAs were employed in two-axis ST systems for PV modules. These trackers were controlled in open-loop with an SPA with GPS. The STEs measured by encoders were ±0.5° and ±0.1°, respectively. The power generation was respectively 26.9% and 40.7% more than a fixed-tilt PV system during clear conditions. Finally, Bedaouche et al. (2017) performed the simulation of a PID control with self-tuning fuzzy logic for ASTS. The step response between the classical PID and the control proposed was shown. The authors mentioned that the proposed control achieved high ST precision, but the STE is not indicated.

It is well known that ease of implementation is one of the main requirements of CAs for ASTS. There are some studies that employ modern CAs for solar trackers: parametric optimization (Alexandru, 2013), fuzzy logic control (FLC) (Alata et al., 2005; Fernandez-Prieto et al., 2020), an adaptive neural fuzzy inference system (ANFIS) (AL-Rousan et al., 2020) and a predictive model (Ikhwan et al., 2018). These controllers aim to achieve greater ST precision, robustness against disturbances and lower energy consumption. All the modern CAs mentioned were programmed on a PC under the MATLAB environment because it has toolbox that facilitates the control system's implementation. Nevertheless, in practice, it is neither economically nor technically feasible to have a PC on ASTS. The implementation of these controllers in a microprocessor or in a PLC would increase complexity.

3.2. Closed-loop solar tracking strategy

This strategy is considered closed-loop because of the control feedback of the Sun's apparent position with a solar sensor. Its block diagram is illustrated in Fig. 6. From the beginning, it is necessary to establish a closed-loop set point, typically equal to 0 for ASTS that use solar sensors based on photosensor arrays or the center of an image (0,0) for a solar sensor based on images. Most of the closed-loop ST systems use a photosensor array, according to Salgado-Conrado (2018). With the established set point and the Sun's position measured by the solar sensor (SP_{Sensor}), it is possible to calculate the $STE_{ClosedLoop}$ using Eq. (2):

$$STE_{ClosedLoop} = 0 - SP_{Sensor}. \quad (2)$$

After that process, the $STE_{ClosedLoop}$ is used as the input of a CA that calculates the desired zenith/azimuth solar angles of the tracker. This

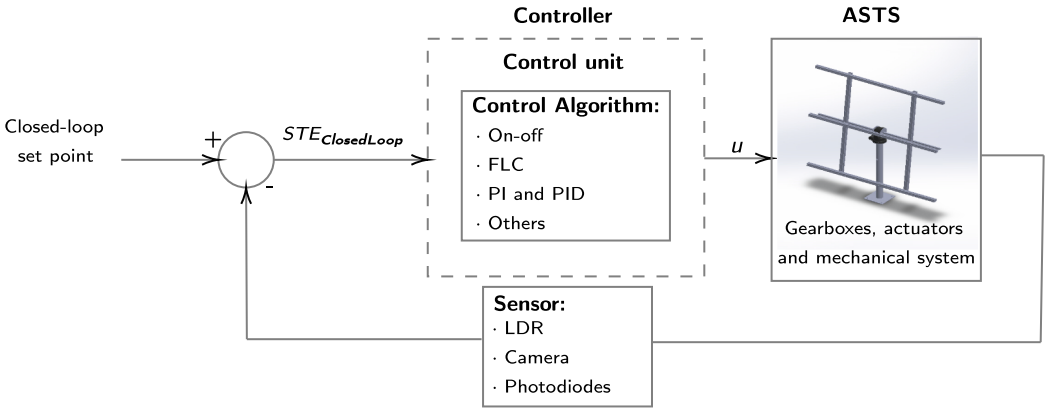

Fig. 6. Block diagram of a conventional closed-loop ST strategy applied to ASTS.

algorithm is implemented in a control unit, generally a PC, μC, FPGA, Arduino, or Raspberry Pi. Finally, these angles are assigned to the actuators of the ASTS to orient the system perpendicularly to the solar rays. The main advantage of the closed-loop strategy is that it achieves higher ST precision than open-loop systems because of feedback control by using a solar sensor. The sensor, however, is susceptible to weather disturbances and solar diffuse irradiance. Table 5 summarizes some advantages and disadvantages found in the works of Luque-Heredia et al. (2004), Khalil et al. (2017), Satué et al. (2020).

One of the main limitations of a closed-loop ST strategy is its dependence on the solar sensor used. For example, the Sun's position can only be detected when the sun is within the field of view (FOV) of the solar sensor (Cristobal et al., 2012). Generally, a sensor with a larger FOV (FOV_a in Fig. 7) has lower precision and accuracy compared with a sensor with a smaller FOV (FOV_b in Fig. 7). This is due to noise measurement induced by diffuse horizontal irradiance (DHI) caused by cloudiness or reflections. A solar sensor with a smaller FOV mainly captures direct normal irradiance (DNI) and can achieve higher accuracy. When the Sun is outside the FOV of the sensor because of the ST start time, cloudiness, or control issues, the system will require a prelocation by means of an SPA or another method. This is known as the hybrid-loop ST strategy.

Fig. 8 depicts a typical flow chart of a closed-loop ST strategy applied to ASTS. As mentioned earlier, at the start, it is necessary to measure the Sun's apparent position through a solar sensor ($P_{SunSensor}$) in order to calculate the $STE_{ClosedLoop}$ with Eq. (2). The $STE_{ClosedLoop}$ can then be compared against a predefined hysteresis, generally used in an on–off control. Some CAs do not require a hysteresis: a difference between the upper and lower threshold of the turn-off and turn-on times of the controller. If the on–off control is used without hysteresis, the system

Table 5
Advantages and disadvantages of the closed-loop ST strategy in ASTS.

Advantages
· It does not require an SPA.
· It achieves high ST accuracy.
· It does not restrict the geographical location.
Disadvantages
· It requires a solar sensor.
· Its operation depends on weather disturbances such as cloudiness or diffuse radiation.
· Solar location is limited to FOV of the solar sensor.
· The complexity and implementation costs of a closed-loop ASTS are higher than in an open-loop system.
· The ST accuracy can be lowered by the use of low precision encoders or solar sensors.
· Most of the photosensors employed in solar sensors do not have a linear response under different temperatures and radiation values.

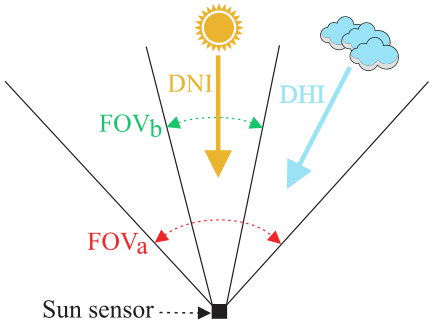

Fig. 7. Comparison between two FOVs from different solar sensors.

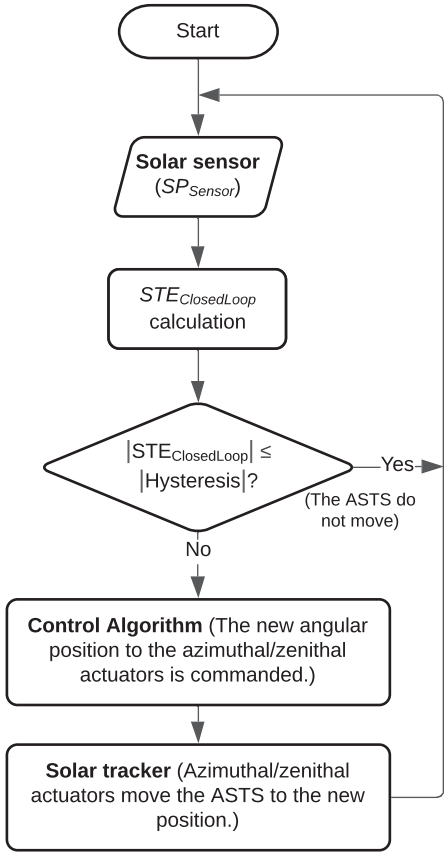

Fig. 8. Flow chart of a closed-loop ST strategy for ASTS.

would produce oscillations/vibrations and increasing energy consumption because of the heating generated, which could fatigue the final control element, for example, causing wear of the motors or in mechanical reduction components. Note that with the use of high reduction gear ratios in the actuators of the ASTS, vibrations/oscillations can probably not be directly observed in the ST. These occur, however, at the motor level, which could affect the useful life of the actuators. Therefore, if the absolute value of $STE_{ClosedLoop}$ is less than or equal to the hysteresis, the ASTS do not move and return to the beginning of the positioning sequence; see the flow diagram. If not, the CA drives the actuators to the new azimuth/zenith position, and the tracker follows the Sun automatically. The ST process continues until the system is aligned perpendicularly to the sunlight, meaning $STE_{ClosedLoop}$ is less than or equal to hysteresis. It is important to mention that a large hysteresis decreases the precision of the ST.

As mentioned above, closed-loop is the most used strategy in ASTS; see Table 2. In this review, a total of 62 manuscripts using this strategy were found, of which 59.68% implement an on–off control, 14.52% an FLC, 3.23% for PI and PID, and 19.34% use other types of controllers. Table 6 shows a summary of control algorithms implemented in closed-loop ST strategies.

Regarding the on–off control works in closed-loop, most of these studies employ signals of low-cost photosensor arrays like photodiodes or light dependent resistors (LDR) to provide feedback for the control system. Because of the simplicity of implementation and low computational cost of this CA, it can be implemented in low-cost embedded systems such as Arduino or even on a conventional μC. Several works have used an Arduino as a low-cost unit control, such as Morón et al. (2017), Hammoumi et al. (2018), and Jamroen et al. (2020), in which energy production increased by 18%, 36.26% and 44.89%, respectively, with respect to a fixed PV system. Similarly, Motahhir et al. (2019) developed a test bench for a prototype of a two-axis solar tracker system that can be used for research and as a teaching platform. On the other hand, Arturo and Alejandro (2010) and Abdollahpour et al. (2018) implemented an on–off CA closed-loop with feedback by webcams. Their results showed STEs of 0.1° and 0.2°, respectively. The use of a charge-coupled device (CCD) or complementary metal–oxide–semiconductor (CMOS) cameras can avoid some problems associated with weather perturbations like nonlinear response face up different solar radiation levels or temperatures changes, which are presented in other types of sensors such as LDRs or photodiodes. Another study performed by Kribus et al. (2004) proposed a similar CA for a heliostat field with an STE <0.017°. This system acquires, by CCD cameras, images of the receiver to provide control feedback through a comparison of the average brightness of the images. Similarly, Fathabadi (2016a) designed and implemented a two-axis tracker based on an irradiance sensor with an STE of 0.14°. The use of closed-loop on–off control with feedback provided by a solar sensor allowed capturing between 27.7% to 42.7% more energy in different seasons of the year with respect to a fixed PV system. The authors concluded that the closed-loop ST systems are more precise but more complicated and expensive to implement than open-loop ST systems.

The performance of FLCs has been studied by numerical simulations in a closed-loop strategy. Ozuna et al. (2011) and Batayneh et al. (2013) proposed, respectively, a position and speed control of the actuators of the ASTS. These parameters were determined from fuzzy inference tables in the MATLAB/Simulink® environment. After performing various stability tests of the system, it was concluded that its experimental implementation is feasible. Similarly, in the work of Usta et al. (2011) different membership functions were implemented for the FLC design for one-axis ST systems: triangular, Gaussian, Cauchy and bell-shaped. The authors concluded that the triangle membership function has a fast response and low overshoot. The bell-shaped membership function yielded the worst result. Regarding experimental studies, the research presented by Fernandez-Prieto et al. (2020) proposed the design of one fuzzy rule-based controller for an HCPV system that was implemented through the Internet of Things technology approach. In this study, two knowledge-based CAs are compared. The first is based on a pointing device, and the second is based on the measurement of the electrical current generated by HCPV modules. It was concluded that the second showed the best ST performance. Similarly, Hamed and El-Moghany (2012) implemented an FLC in an ST system by a field-programmable gate array (FPGA) in the Matlab/Simulink® environment. This controller employs the Mamdani method, which has three parts: fuzzification, rule-based system, and defuzzification. The PV panel achieved 24% more energy than a fixed PV system. Finally, El-Moghany and Hamed (2012) and Yan and Jiaxing (2010) employed FLCs programmed in a μC for closed-loop ST systems in order to reduce the energy consumption of the motors. The last work showed an increase in the energy generated by a PV module of 22.5% compared with a fixed PV system. All mentioned FLC works use photosensor arrays to provide the control feedback.

Classic control is also used in closed-loop ST strategies. Carballo et al. (2018) developed an ST system learning tool that uses a Raspberry Pi camera module to calculate the Sun's position. This learning tool employs a PI CA in the Mathematica® and Simulink® environments. Because of its flexibility, this system allows the user to experiment with image processing algorithms and CAs applied to ASTS. Similarly, Sabir and Ali (2016) simulated a PID controller for a two-axis ST system in MATLAB/Simulink®. This controller design was formulated as an optimization problem, and the tuning was performed using algorithms based on swarm intelligence. Another simulation study of a PID CA for two-axis ST systems was proposed by Oladayo and Titus (2016). In this work, the tuning of the controller was carried out by an internal model control (IMC) in the MATLAB® environment. The results obtained showed a fast, stable response and low overshoot in the ST; therefore, it was concluded that the IMC strategy is an effective tool for optimizing PID control.

As shown in Table 6, some works use modern CAs to command and manipulate the electrical signals to the actuators of the ASTS. Regarding experimental studies, in the work of Aldair et al. (2016), a neuro-fuzzy logic controller was developed and implemented using an FPGA for a two-axis ST system with linear actuators. Experimental results showed that this controller is more robust than the FLC and the PI controller. This system was capable of collecting 50.6% more daily energy than a fixed PV panel. Similarly, Garrido and Díaz (2016) proposed a cascade CA for a one-axis ST prototype with an STE of 0.014°. This control used a scheme with an internal and external nonlinear classic control. There are other interesting studies that employed modern CAs using numerical simulations: SMC, in which an equivalent control approach using a low-pass filter permitted the reduction of the chattering effects (Díaz et al., 2018); the linear quadratic regulator (LQR), where simulation results showed that it is feasible to apply it to a real system (Mazumdar et al., 2015); robust control, in which the effective rejection of constant disturbances was demonstrated (Limon et al., 2008); and finally machine learning, where the managing sensor data dynamics compared with other machine learning techniques was demonstrated (Mustafa et al., 2019).

3.3. Hybrid-loop solar tracking strategy

In recent years, because of the tracking accuracy requirements in CSP and HCPV systems, some authors have presented innovative proposals that have the advantages of both open-loop and closed-loop ST strategies by combining them, which is commonly known as the hybrid-loop ST strategy. Typically, this strategy is based on two control loops: a coarse control implemented in open-loop and a fine control performed in closed-loop. Both loops are generally not activated at the same time; however, there are studies where weighting algorithms are used between both loops to calculate the control signal of the solar tracker (Safan et al., 2017). It is important to mention that the control algorithms of both control loops could be different, as in the study of the

Table 6
Summary of closed-loop control algorithms applied to ASTS.

N	Authors	Exp./ Sim.	Control algorithm	ST accuracy	Axis	Motor type	Sun localization	Control Unit
1	Morón et al. (2017)	Exp.	On–off	-	Two	Linear and stepper	Photodiodes	Arduino
2	Arturo and Alejandro (2010)	Exp.	On–off	0.1°	Two	DC	Webcam	PC MATLAB
3	Barker et al. (2013)	Exp.	On–off	-	Two	Linear	Photodiodes	PC
4	Hoffmann et al. (2018)	Sim.	On–off	-	Two	DC	LDR	µC
5	Wang and Lu (2013)	Exp.	On–off	-	Two	AC	LDR	-
6	Wei et al. (2016)	Exp.	On–off	-	Two	Servomotor	PiCamera NoIR + Lens	PC/Raspberry Pi
7	Abouzeid (2001)	Sim.	On–off	7.5°	One	Stepper	Photo-sensing cells	EEPROM and PLA
8	Su et al. (2018)	Exp.	On–off	-	Two	-	Photosensors	PC
9	Sefa et al. (2009)	Exp.	On–off	-	One	DC	LDR	PC and µC
10	Chin et al. (2011)	Exp.	On–off	-	One	Servomotor	LDR	PC and µC
11	Aracil et al. (2006)	Exp.	On–off	-	Two	DC	Photodiodes	µC
12	Yilmaz et al. (2015)	Exp.	On–off	-	Two	DC	LDR	µC
13	Skouri et al. (2016)	Exp.	On–off	< 0.2°	Two	DC	LDR	µC and PLC
14	Makhija et al. (2017)	Exp.	On–off	-	Two	Servomotor	LDR	µC
15	Fathabadi (2016a)	Exp.	On–off	0.14°	Two	Stepper	Irradiance sensor	µC
16	Kivrak (2013)	Exp.	On–off	-	One	DC	PV panel	Basic electronics
17	Abdollahpour et al. (2018)	Exp.	On–off	2°	Two	Stepper	Webcam	Arduino
18	Stamatescu et al. (2014)	Exp.	On–off	-	Two	DC	Four photosensitive cells	LabVIEW
19	Berenguel et al. (2004)	Exp.	On–off	-	Two	Servomotor	Camera	PC
20	Kribus et al. (2004)	Exp.	On–off	<0.017°	Two		Camera	PC
21	Roos et al. (2008)	Exp.	On–off	0.19°	Two	DC	Phototransistors	-
22	Jamroen et al. (2020)	Exp.	On–off	-	Two	DC	LDR	µC Arduino
23	Mohammad and Karim (2013)	Exp.	On–off	-	Two	Stepper	Photosensors	µC
24	Chowdhury et al. (2019)	Exp.	On–off	0.6°	Two	Servomotor	LDR	µC
25	Mahmood and Muhammed (2010)	Exp.	On–off	7.5°	Two	DC	LDR	Smart relay
26	Mousazadeh et al. (2011)	Exp.	On–off	-	Two	DC	LDR	µC
27	Normanyo and Awingot (2016)	Sim.	On–off	-	Two	Stepper	-	µC
28	Arbab et al. (2009)	Exp.	On–off	-	Two	DC	Photosensor/camera	µC
29	Kumar and Arjun (2016)	Sim.	On–off	-	One	DC	LDR	PLC
30	El Kadmiri et al. (2015)	Exp.	On–off	-	Two	DC	CCD	µC
31	Ghassoul (2018)	Exp.	On–off	-	One	DC	LDR	µC
32	Hammoumi et al. (2018)	Exp.	On–off	-	Two	Servomotor	LDR	µC Arduino
33	Motahhir et al. (2019)	Exp.	On–off	-	Two	Servomotor	LDR	µC Arduino
34	Akbar et al. (2017)	Exp.	On–off	-	Two	DC	LDR	µC Arduino
35	Okandeji et al. (2020)	Exp.	On–off	1.5°	One	DC	LDR	µC
36	Hasanah et al. (2020)	Exp.	On–off	-	One	DC	LDR	µC and PC
37	Sneineh and Salah (2019)	Exp.	On–off	-	Two	DC/linear	LDR	µC
38	Mustafa et al. (2019)	Exp.	Machine Learning	-	Two	-	LDR	PC
39	Carballo et al. (2018)	Exp.	PI	-	Two	DC	Camera	PC and Raspberry Pi
40	Flores-Hernández et al. (2017)	Exp.	GPI	-	Two	DC	Photodiode array	µC
41	Sabir and Ali (2016)	Sim.	PID	-	Two	DC	-	PC Simulink
42	Oladayo and Titus (2016)	Sim.	IMC-PID	-	Two	DC	LDR	PC MATLAB
43	Yazidi et al. (2006)	Exp.	PID	-	One	DC	PV sensors	PC LabVIEW
44	Ontiveros et al. (2020)	Sim/ Exp.	PID/FLC	-	Two	DC	SPA and gyroscope	PC and µC
45	Kiyak and Gol (2016)	Sim.	PID-FLC	-	One	DC	LDR	PC and µC
46	Keshtkar et al. (2016)	Sim.	Adaptive SMC	-	Two	linear	Photosensors	PC Simulink
47	Yan and Jiaxing (2010)	Exp.	FLC	-	Two	Stepper	Four-quadrant photodiodes	µC
48	Ozuna et al. (2011)	Sim.	FLC	-	Two	DC	LDR	PC Simulink
49	Usta et al. (2011)	Sim.	FLC	-	-	DC	Photosensors	PC Simulink
50	Batayneh et al. (2013)	Sim.	FLC	-	Two	DC/linear	Four photosensors	PC MATLAB
51	Fernandez-Prieto et al. (2020)	Exp.	FLC	0.10°/0.45°	Two	-	Four-quadrant of LDR	µC
52	Fernandez-Prieto et al. (2020)	Exp.	FLC	0.91°/0.27°	Two	-	Electrical current generated by HCPV modules	µC
53	El-Moghany and Hamed (2012)	Exp.	FLC	-	Two	Stepper	LDR	µC and Simulink
54	Hamed and El-Moghany (2012)	Exp.	FLC	-	One	Stepper	LDR	FPGA-Simulink
55	Huang et al. (2016)	Exp.	FLC	-	Two	Stepper	Photodetector	PC

(*continued on next page*)

Table 6 (*continued*)

N	Authors	Exp./ Sim.	Control algorithm	ST accuracy	Axis	Motor type	Sun localization	Control Unit
56	Aldair et al. (2016)	Exp.	Neuro-Fuzzy Logic	-	Two	DC linear	Photosensors	FPGA
57	Carballo et al. (2019)	Exp.	Neural network	0.17°	Two	-	Camera	Raspberry Pi
58	Shenawy et al. (2012)	Sim.	Neural network/ FLC-PID	-	Two	-	-	PC
59	Díaz et al. (2018)	Sim.	SMC	-	Two	DC linear	-	PC Simulink
60	Garrido and Díaz (2016)	Lab.	Cascade	0.014°	One	Servomotor	Photodiodes	PC Simulink
61	Mazumdar et al. (2015)	Sim.	LQR	-	Two	DC	-	PC Simulink
62	Limon et al. (2008)	Sim.	Robust control	-	One	-	Pyrometer	PC

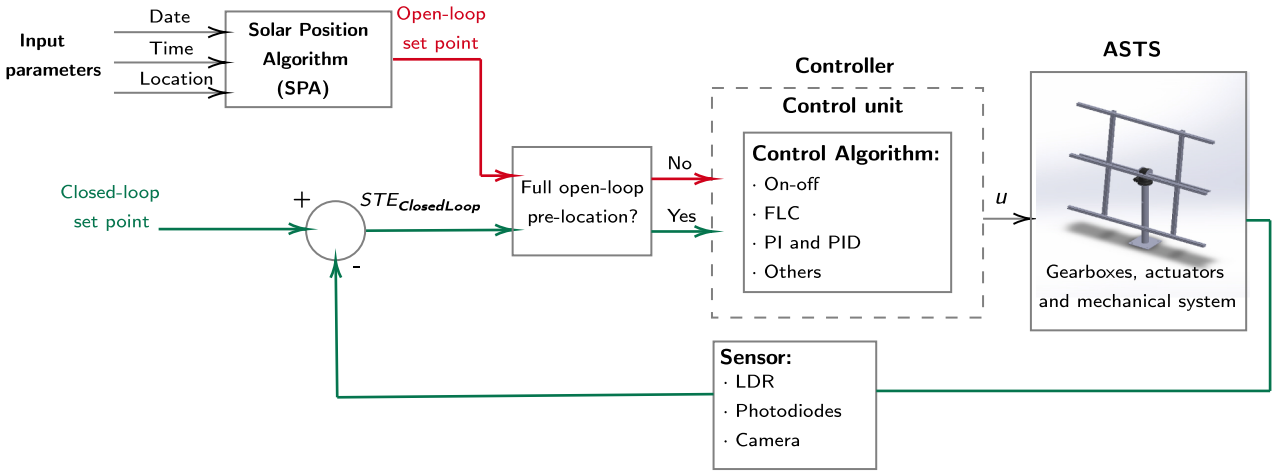

Fig. 9. Block diagram of a conventional hybrid-loop ST strategy applied to ASTS.

work of Yeh and Lee (2012).

Fig. 9 depicts a block diagram of a typical ST hybrid-loop. This figure shows that there are two possibilities for establishing the reference or set point of the control system: one in open-loop mode (red line) and another one in closed-loop mode (green line). The control unit has the ability to switch in real-time between both modes depending on whether the pre-location of the solar tracker has been completed. After this process, the CA programmed in the control unit generates a control signal u to move the actuators. Fig. 10 simulates the behavior of a hybrid-loop strategy during a day (from 8 h to 18 h). For simplicity, just the azimuth axis was considered; the azimuth angles of the Sun are the only representative. The details of the tracking modes of this tactic are described below.

- Open-loop mode. Commonly, this control implements an SPA for estimating the Sun's apparent path in order to generate a set point to initially pre-locate the tracker. This tracking mode is executed when the solar tracker position is not within the allowed tracking hysteresis, which is established according to the allowed STE of the solar energy harvesting system or by the FOV of the solar sensor used in

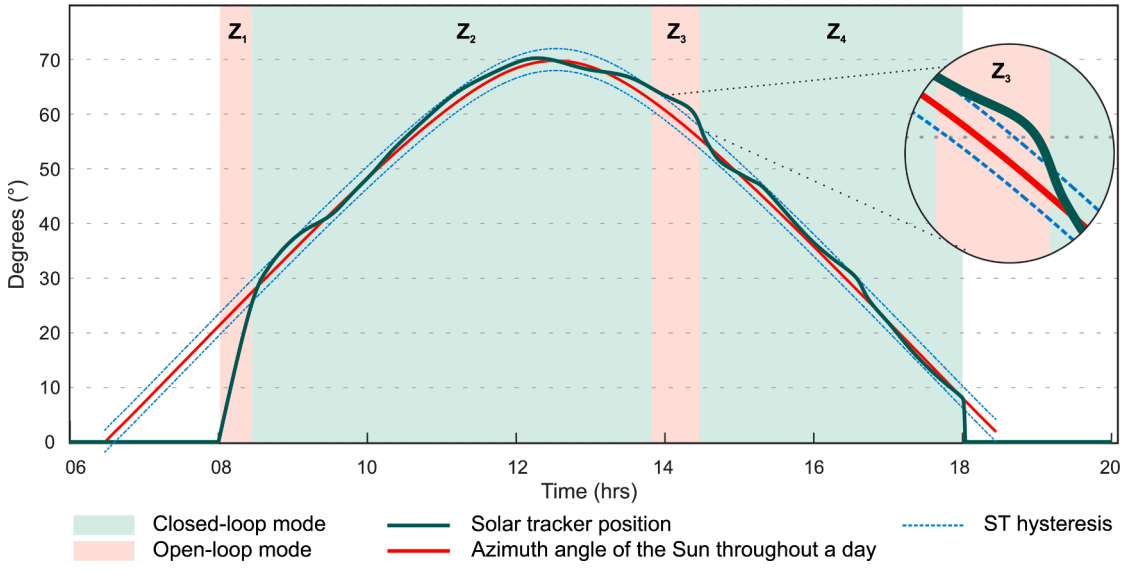

Fig. 10. Solar location method using the hybrid ST strategy.

the closed-loop. There are two situations when this ST mode is activated: 1) at the start of solar tracking at sunrise and 2) when the device used as a solar sensor is not capable of detecting the position of the Sun, as is the case of cloudiness. When starting the tracking system, the tracker must perform an initial pre-location as can be seen in Z_1 zone of Fig. 10. Throughout the day, even when the ST is executed in closed-loop mode, the tracker position can leave of the hysteresis, as observed in the Z_3 zone of Fig. 10, which disables the closed-loop and activates open-loop tracking. Because of all the factors that affect the open-loop strategy described in Section 3.1, its tracking accuracy is low; therefore, after pre-locating, the control unit switches to a closed-loop tracking mode.

- Closed-loop mode. Generally, because of their low cost and ease of implementation, this control mode employs solar sensors based on four-quadrant photosensors like LDRs or photodiodes to feedback the control loop; however, some authors use cameras or the energy generated in the PV cells or modules. After open-loop mode, when the solar tracker position is within the allowed tracking hysteresis, the control unit turns the open-loop mode off, and the closed-loop mode establishes a fine set point to correct the solar tracker position, as is shown in Z_2 and Z_4 zones of Fig. 10.

The main pros and cons of a hybrid-loop strategy are presented in Table 7. This strategy is not affected by factors that decrease the ST precision, such as the installation deviation of the tracker, errors in the estimation of the Sun's position by the SPA, and errors caused by the weather conditions, among others. These ASTS with a hybrid-loop control do not need a precise procedure of installation or recalibration. Accordingly, this strategy presents greater reliability, performance and tracking accuracy than open- and closed-loop ST strategies so that it is commonly used in CPV or HCPV systems, where the performance decreases drastically with small solar tracking errors. Note that in this control strategy, as in open- and closed-loop, it is necessary to consider the energy-saving factors to avoid overconsumption of energy by unnecessary reorientation of the solar tracker. Therefore, the frequency and tolerance of solar tracking will depend on the cost-benefit relationship of each solar energy harvesting system.

In order to emphasize the principle of operation of a hybrid-loop ST strategy, Fig. 11 shows a flow chart of a typical hybrid strategy that employs an SPA in the open-loop to make the coarse control, and a solar sensor feeds back to the closed-loop to perform the fine control. A number is assigned to each process condition to facilitate the explanation.

P1. At the initiation of the ST, as with the open-loop strategy, it is necessary to know the parameters for locating the Sun's position using an SPA. These can be entered manually or generated by GPS.

P2. Next it is necessary to verify if the full open-loop pre-location is done. In the case that the pre-location has finished, the system continues to the process P3. Generally, the pre-location is considered finished through two methods: 1) When the Sun's position is within the $FOV_{SunSensor}$ as seen in Fig. 10 and the solar sensor generates enough current or voltage and 2) when the $STE_{OpenLoop}$ is less than a prespecified value in the control system (it requires a position sensor). If the pre-location process has not finished, however, the system passes to the ST process P6.

P3. In this process condition, the ASTS start operating in closed-loop. The Sun's position is calculated by processing the signals obtained from a solar sensor (SP_{Sensor}).

P4. Using the solar sensor signals, the system verifies that solar radiation is sufficient for operating in closed-loop. If the solar sensor does not receive enough solar radiation because of an occlusion caused by a cloud, the system reverts to P1. This strategy ensures that even under cloudy conditions the ST system can continue to function through calculating the Sun's position with the SPA.

P5. The system calculates the $STE_{ClosedLoop}$ with Eq. (2). It is generally compared with a predefined hysteresis to reduce energy consumption in the ST. If the $STE_{ClosedLoop}$ is less than or equal to the hysteresis, the system returns to P3. In CAs where there is no hysteresis, only the $STE_{ClosedLoop}$ is calculated and continues in the following process stage.

P6. ST process. There are two ways to reach to this process condition.
a. From P2 (open-loop). A set point is established with an SPA. The CA commands the new angular position, and the azimuthal/zenithal actuators move the solar tracker to the new position. After this process, the system returns to P1 to continue the open-loop ST.
b. From P5 (closed-loop). The set point is generally set equal to 0. The CA commands the new angular position, and the actuators move the solar tracker to the new position. After this process, the system returns to P3 to continue the closed-loop ST.

Table 7
Advantages and disadvantages of the hybrid-loop ST strategy.

Advantages
· ST precision and accuracy are generally high.
· ST can be performed even under cloudy conditions.
· It does not require continuous calibration.
Disadvantages
· It requires the location, time, date and orientation of the ST system.
· Its implementation is more expensive and complex than open- and closed-loop ST systems.
· It requires an SPA.
· It requires a solar sensor.

From the works considered in this review, 16.67% use a hybrid ST strategy as seen in Table 2, of which 47.37% implement an on–off control, 15.79% a PID, 10.53% a PI control and 26.31% other types of CAs as shown in Table 8. As in the case of open- and closed-loop the on–off CA is the most widely used algorithm in the hybrid ST strategy because of its ease and low-cost implementation. In the works of Yao et al. (2014), Burhan et al. (2016), Song et al. (2013), Zhang et al. (2019) and Liu et al. (2017), the authors proposed several ST strategies using an innovative photosensor array. These studies achieved STEs of 0.15°, <0.3°, 0.1°, <0.91°, and 0.5°, respectively. It is important to emphasize that most of the time these studies lack the methodology for estimating ST. Similarly, a study of Ferdaus et al. (2014) presented a hybrid two-axis ST system controlled by an on–off CA that generated 25.62% more average power than a fixed PV system and the same energy as a continuous ST system based on an LDR array. The power saved in the hybrid system, however, was 44.44% higher than in the continuous ST. Finally, another study uses the second derivative of the produced energy for the optimal movement of a one- and two-axis ST system (Seme et al., 2016). The authors mention that the proposed method can achieve a higher annual energy production of up to 2% as compared with the closed-loop ST systems with a tracking frequency every 2 h.

Classic CAs are used in hybrid strategies because of their ease of implementation and tuning. Rubio et al. (2007) presented a strategy based on an SPA as coarse control and dynamic feedback as fine control. This work used a PI controller with an experimental STE of 0.15°, and the achieved energy increase compared with an open-loop ST strategy was 40%. In addition, the same authors designed and implemented an error-correcting routine to substitute the PI controller of the previous work (Luque-Heredia et al., 2004). On the other hand, in the work of Mao et al. (2018) a PID controller is employed in a hybrid system that uses an SPA feed by a GPS and a four-quadrant of photosensors. The reported STE was 0.15°. In the same way, an MDOF-SUI PID controller

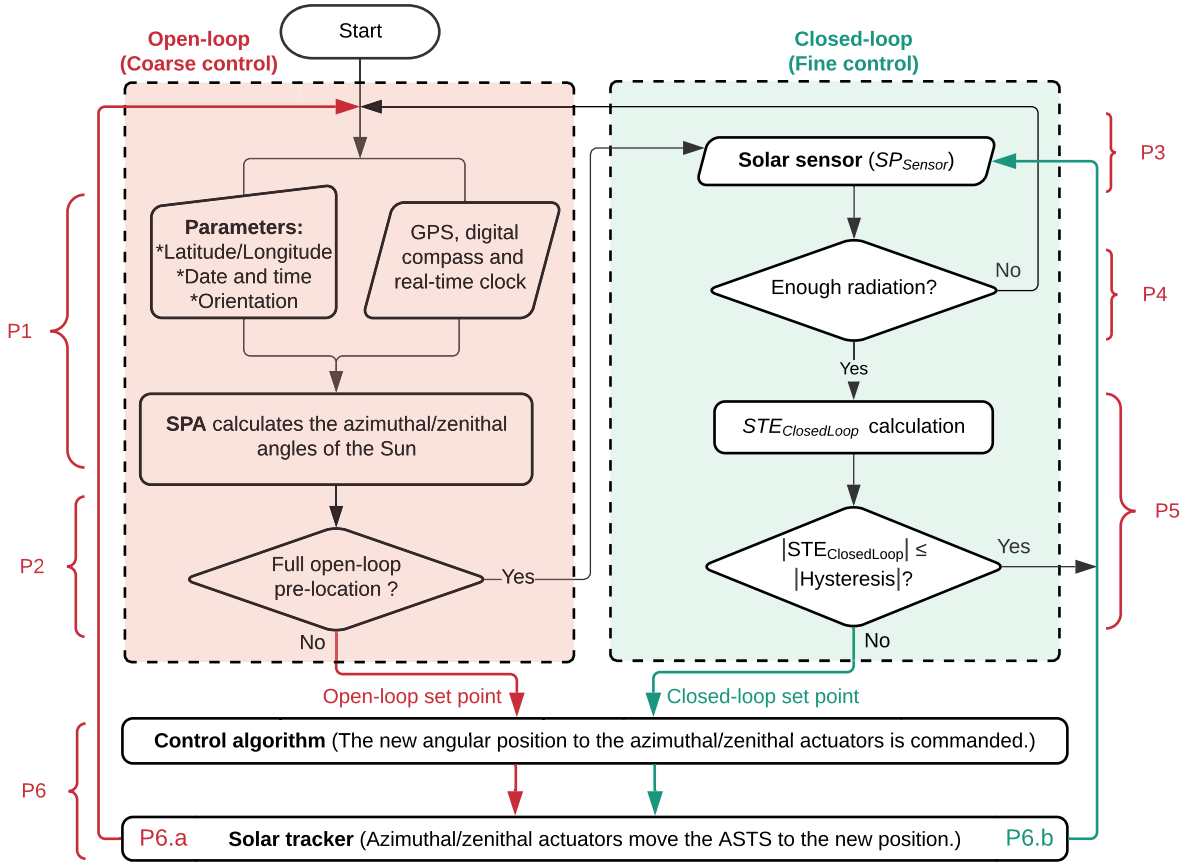

Fig. 11. Flow chart of a typical hybrid-loop ST strategy applied to ASTS.

Table 8
Summary of hybrid-loop control algorithms applied to ASTS.

N	Authors	Exp./ Sim.	Control algorithm	ST accuracy	Axis	Motor type	Sun localization	Control Unit
1	Yao et al. (2014)	Exp.	On–off	0.15°	Two	Linear	SPA and four-quadrant photocells	μC-Control,PC-Monitoring
2	Roth et al. (2004)	Exp.	On–off	-	Two	DC	SPA and four-quadrant photodiode	μC
3	Burhan et al. (2016)	Exp.	On–off	< 0.3°	Two	Stepper	SPA and photosensors	μC
4	Zhang et al. (2019)	Exp.	On–off	< 0.91°	Two	Stepper	SPA with GPS/BeiDou and four-quadrant photosensors	μC
5	Song et al. (2013)	Exp.	On–off	0.1°	Two	Stepper	SPA with GPS and photodiode matrix	μC
6	Liu et al. (2017)	Sim.	On–off	-	Two	DC	SPA and sun sensor	PC MATLAB
7	Seme et al. (2016)	Exp.	On–off	-	One and two	-	SPA and photovoltaic system	PC
8	Kang et al. (2019b,a)	Exp.	On–off	-	Two	-	SPA and climate sensor	PC LabVIEW
9	Jianwattananukul et al. (2016)	Exp.	On–off	±2°	Two	DC	SPA and LDR	μC
10	Rubio et al. (2007)	Exp.	PI	-	Two	-	SPA and a photovoltaic arrays	μC and PC LabVIEW
11	Luque-Heredia et al. (2004)	Sim.	PI	-	Two	DC	SPA and a sensor lacking directional information	PC Simulink
12	Mao et al. (2018)	Exp.	PID	0.15°	Two	Stepper	SPA with GPS and photodetector	μC
13	Xie et al. (2019)	Sim.	PID	-	Two	Stepper	SPA and CCD	PC
14	Safan et al. (2017)	Sim.	MDOF-SUI PID	±0.2°	Two	Stepper	SPA and solar sensor	PC MATLAB
15	Hammad et al. (2014)	Sim.	Adaptive control	-	Two	-	SPA and solar sensor	PC MATLAB
16	Kim and Cho (2019)	Sim.	Bayesian Network	-	-	-	SPA/Camera	PC-MATLAB
17	Azizi and Ghaffari (2013)	Exp.	FLC	< 0.15°	Two	DC	LDR and webcam	MATLAB
18	Alorda et al. (2015)	Exp.	Distributed control	-	One	DC	SPA and a photovoltaic cell	μC
19	Yeh and Lee (2012)	Exp.	Logig-based supervisor/PID	±0.2°	Two	DC	SPA and a solar sensor	μC

for an ST system was simulated in the MATLAB/Simulink environment (Safan et al., 2017). The controller output is established by a weighing equation of the coarse control performed by an SPA and the fine control carried out with a solar sensor.

Recently, the performance of the hybrid ST systems driven by modern CAs has also been studied. Hammad et al. (2014) simulated the performance of a hybrid strategy through an SPA and with feedback from a Sun position sensor. This work employs an adaptative control for driving the actuators, showing a quick convergence. In the research of Kim and Cho (2019), a CPV system with ST through four methods for calculating the Sun's position was proposed, which is selected by a weather recognition Bayesian network. Three of these algorithms are based on the digital processing of images acquired by a pinhole webcam, and the fourth algorithm uses an SPA to estimate the Sun's position. The work of Azizi and Ghaffari (2013) presented an FLC with an STE $< 0.15^{\circ}$ where the coarse control is made by LDRs and the fine control by a method of processing images acquired with a camera. When the solar radiation level is not great enough, the authors consider an energy-saving mode in which an ST delay is made and the system holds the last position. Finally, a novel fixed mirror solar concentrator is presented by Alorda et al. (2015). In this study, the collector is moved to receive the solar radiation reflected in the fixed mirrors through a one-axis ST driven by a collaborative distributed control that tries to maintain the maximum energy conversion efficiency in the system. The hybrid strategy was performed by an SPA and fine-tuning algorithm that searches the optimal position in order to capture the maximum flux concentration. This system was implemented as a controller area network (CAN) distributed system. It is important to emphasize that in any ST strategy it is more complicated to implement a modern CA than a classic CA. Therefore, some of the modern CAs studied in the literature have only been reported in numerical simulations.

4. Alternative classification of control algorithms applied to ASTS

The control unit's selection depends on different factors, such as their processing speed, cost, autonomy, power consumption, availability in the market, programming complexity, among others, and there are two main control units for solar trackers: PCs and μCs. Fig. 12 shows an alternative classification of CAs applied to ASTS taking into account their control unit. This figure depicts that computational simulation works are mainly performed using MATLAB/Simulink and LabVIEW, which have specific toolboxes for control systems that facilitate the programming, characterization and performance analysis of the system. The main disadvantage of a PC is its lack of autonomy and high cost. In the same way, the μCs and PCs are the main control units for experimental studies. As far as classic CAs are concerned, the on–off control has been practically executed in any control unit: PCs, μCs, electronic basics, PLC, Raspberry Pi, Arduino, PLA and smart relay. PI and PID algorithms are regularly run on μCs or PCs because they require a higher processing speed and their complexity is higher than the on–off control. The execution of these algorithms in μCs requires the discretization of signals, which makes its implementation relatively more complex. The suitable control units for classic algorithms could be the μCs and low-cost embedded systems due to the ease of programming, low cost, autonomy, low energy consumption and high availability and variety in the market. On the contrary, modern CAs are not implemented in low-cost embedded systems because of their high programming complexity and the high computational capacity required; these CAs are suitable to being programmed in μCs or PCs.

5. Discussion

The total STE is the sum of the errors caused by factors conditioning ST precision in ASTS (see Table 1). Typically, in the literature, only the error reached by the CA is reported, and its methodologies are often unclear or are obtained without the consideration of the IEC:62817 qualification standard that is applicable to solar trackers. This review demonstrates the need to implement this standard in order to objectively compare the precision and accuracy of CAs applied to ASTS for better comparison and validation of the ST algorithms. In addition, the IEC:62817 standard should be frequently updated to include all types of ST systems and new developments.

As shown in Table 1, there are several factors that can limit the precision of ST and, therefore, decrease the energy conversion efficiency of the solar energy generation systems with ST. One of the simplest, fastest and cheapest ways to increase energy conversion efficiency is to modify the software-defined components. The performance of ASTS can be considerably better/worse if only the CA and/or its tuning parameters are changed. The ST strategy and the CA should be selected according to the system requirements. The response of the ST system should be robust against disturbances and possess high repeatability and

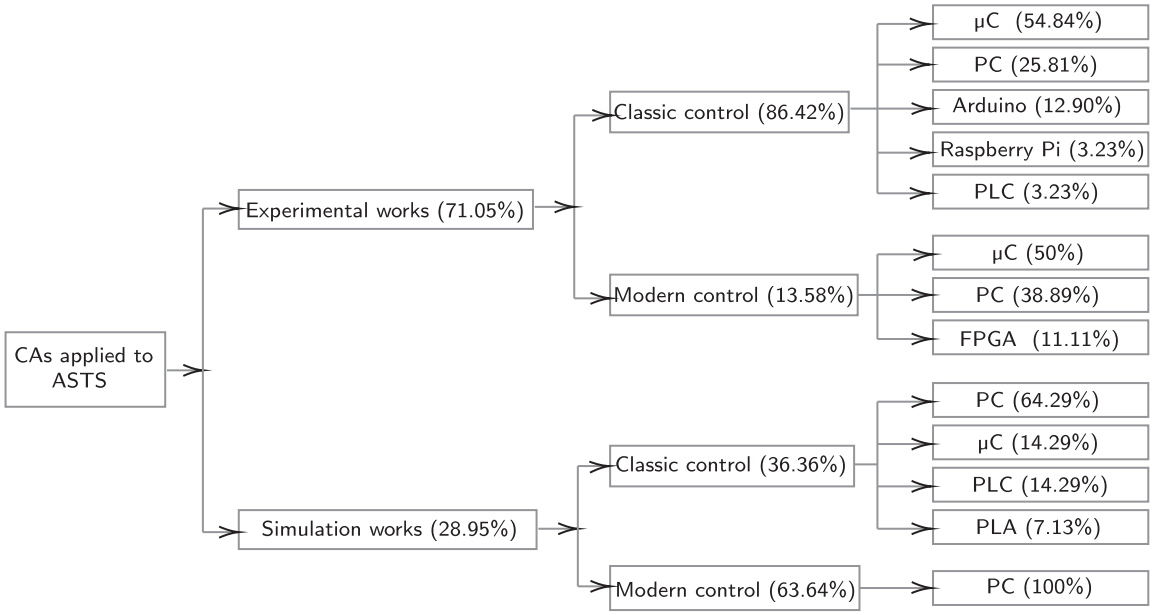

Fig. 12. Alternative classification of CAs applied to ASTS based on the control units.

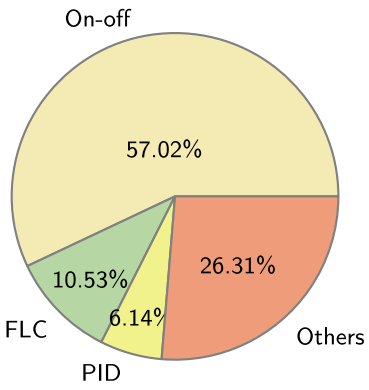

Fig. 13. Most common control algorithms applied to ASTS.

precision.

From studies considered in this review, 73.69% focus on the use of only three CAs as seen in seen Fig. 13 (on–off, FLC, and PID), regardless of their ST strategy. It is important to know in advance the characteristics of the system that will be installed in the ST system, especially its acceptance angle, in order to establish the tolerance of STE in performing the optimal mechatronic design of the solar tracker according to the needs. In addition, knowing the tolerance of STE of the system allows us to select the ST strategy and the most suitable CA. It is also important to consider, however, the power consumption, the cost, the difficulty of construction and the maintenance required.

In order to achieve a good cost-benefit relationship in ASTS, it is important to consider the characteristics and costs of the control units. One of the most important factors for the selection of this element is the complexity of the implementation of the control algorithms. Classic CAs with a low programming complexity that do not require high computational capacity are typically implemented in μCs or PCs; however, they can be easily programmed in low-cost embedded systems such as Arduino and Raspberry Pi. Modern CAs are suitable for μCs or PCs because of their high programming complexity and the high computational capacity required. Although it is typically desirable that the CAs applied to ASTS be easy to implement, some authors justify the use of more complex modern CAs because these controllers could offer advantages, such as greater robustness to external disturbances, greater ST accuracy, smoother control signals and/or greater stability control. Most of these controllers, however, have only been studied in numerical simulations.

In the case of CPV modules, there is a trend towards the ultra-high CPV system with the aim of increasing efficiency and reducing energy production costs. These systems, however, require higher precision and accuracy in ASTS, so developing more accurate and low-cost ST systems is mandatory.

6. Conclusion

In this paper, a review of different CAs applied to ASTS was presented. These were classified according to their control strategy: open-loop, closed-loop and hybrid-loop. The following conclusions can be drawn from this work.

- From works considered in this paper, 54.39% implement a closed-loop control strategy, 28.95% an open-loop, and 16.67% a hybrid-loop strategy. Most of the open-loop ST systems are inappropriate for CSP and CPV because of their low tracking precision. In recent years, innovative hybrid-loop control strategies have been proposed to achieve greater precision in the ST system and, consequently, to increase energy production.
- The most used CAs in ASTS are the on–off, fuzzy logic, PID, and PI controls, which represent a total of 57.02%, 10.53%, 6.14%, and 4.39%, respectively. The on–off CA is implemented in 57.58%, 59.68%, and 47.37% of the open-loop, closed-loop, and hybrid-loop strategies, respectively. The response of the CA must be robust against disturbances, with high accuracy ST and stability, with soft control signals and with low power consumption. Furthermore, it is desired that the CA be easy to implement in the control unit.
- Most of the works do not report the achieved solar tracking precision.
- It is necessary to implement test procedures from the IEC:62817 standard to allow a comprehensive comparison and validation of ST systems' performance.
- The control unit's selection for ASTS is mainly based on its cost, autonomy and the complexity of the implementation and computational capacity required of the CAs.
- The main control units for ASTS are μCs because of its low cost. PCs are also used because of the control system toolboxes of MATLAB® and LabVIEW® and the use of data acquisition systems.
- About 70% of the CAs that require a control feedback (closed-loop and hybrid-loop) use photosensor arrays because of their low cost and easy implementation. Some authors, however, report low precision of the ST because of the quality and nonlinearity of some photosensors.
- Despite the large number of CAs applied in the ASTS reported in the literature, there is no optimal CA because of the design differences in the solar trackers. The performance of an ST system can be optimized by taking into account the technical requirements of the solar power generation systems, especially, the acceptance angle of CSP-CPV technology and the cost-benefit relationship.

In conclusion, continuing with the design and implementation of ST strategies and CAs in order to achieve technological maturity in solar energy generation systems is critical. Similarly, in the design of new prototypes of ASTS, it is necessary to achieve a reduction in costs and maintenance, ease of construction and implementation, and greater precision and accuracy of ST.

Declaration of Competing Interest

The authors declare that they have no known competing financial interests or personal relationships that could have appeared to influence the work reported in this paper.

Acknowledgements

Rosa F. Fuentes-Morales wishes to acknowledge CONACyT México for its support by a PhD scholarship.

References

Abdallah, S., Badran, O., 2008. Sun tracking system for productivity enhancement of solar still. Desalination 220, 669–676.
Abdallah, S., Nijmeh, S., 2004. Two axes sun tracking system with plc control. Energy Convers. Manage. 45, 1931–1939.
Abdollahpour, M., Golzarian, M.R., Rohani, A., Zarchi, H.A., 2018. Development of a machine vision dual-axis solar tracking system. Sol. Energy 169, 136–143.
Abouzeid, M., 2001. Use of a reluctance stepper motor for solar tracking based on a programmable logic array (pla) controller. Renewable Energy 23, 551–560.
Aipperspach, W., Bambrook, S., Trujillo, P., Zech, T., Berenguel, F.R., 2015. Evaluation of the iec 62817 mechanical testing for the tracker validation. In: AIP Conference Proceedings. AIP Publishing, p. 080001.
Akbar, H.S., Siddiq, A.I., Aziz, M.W., 2017. Microcontroller based dual axis sun tracking system for maximum solar energy generation. Am. J. Energy Res. 5, 23–27.
AL-Rousan, N.A., Isa, N.A.M., Desa, M.K.M., 2020. Efficient single and dual axis solar tracking system controllers based on adaptive neural fuzzy inference system. J. King Saud Univ.-Eng. Sci.
Alata, M., Al-Nimr, M., Qaroush, Y., 2005. Developing a multipurpose sun tracking system using fuzzy control. Energy Convers. Manage. 46, 1229–1245.
Aldair, A.A., Obed, A.A., Halihal, A.F., 2016. Design and implementation of neuro-fuzzy controller using fpga for sun tracking system. Iraqi J. Electrical Electronic Eng. 12, 123–136.
Alexandru, C., 2013. A novel open-loop tracking strategy for photovoltaic systems. Scientific World J. 2013.

Alexandru, C., Pozna, C., 2010. Simulation of a dual-axis solar tracker for improving the performance of a photovoltaic panel. Proc. Inst. Mech. Eng., Part A: J. Power Energy 224, 797–811.

Allil, R.C., Manchego, A., Allil, A., Rodrigues, I., Werneck, A., Diaz, G.C., Dino, F.T., Reyes, Y., Werneck, M., 2018. Solar tracker development based on a pof bundle and fresnel lens applied to environment illumination and microalgae cultivation. Sol. Energy 174, 648–659.

Alorda, B., Pujol-Nadal, R., Rodriguez-Navas, G., Moià-Pol, A., Martínez-Moll, V., 2015. Collaborative distributed sun-tracking control system for building integration with minimal plant area and maximum energy-conversion efficiency. Int. J. Electrical Power Energy Syst. 70, 52–60.

Aracil, C., Quero, J., Castaner, L., Osuna, R., Franquelo, L., 2006. Tracking system for solar power plants, in. In: IECON 2006-32nd Annual Conference on IEEE Industrial Electronics. IEEE, pp. 3024–3029.

Arbab, H., Jazi, B., Rezagholizadeh, M., 2009. A computer tracking system of solar dish with two-axis degree freedoms based on picture processing of bar shadow. Renewable Energy 34, 1114–1118.

Arturo, M.M., Alejandro, G.P., 2010. High-precision solar tracking system. In: Proceedings of the World Congress on Engineering, pp. 844–846.

Arul Kumar, M., Arjun, T., 2016. Design of single axis solar tracking system using plc. Middle-East J. Scientific Res. 24, 1–5.

Awasthi, A., Shukla, A.K., SR, M.M., Dondariya, C., Shukla, K., Porwal, D., Richhariya, G., 2020. Review on sun tracking technology in solar pv system. Energy Reports 6, 392–405.

Azizi, K., Ghaffari, A., 2013. Design and manufacturing of a high-precision sun tracking system based on image processing. Int. J. Photoenergy 2013.

Barker, L., Neber, M., Lee, H., 2013. Design of a low-profile two-axis solar tracker. Sol. Energy 97, 569–576.

Batayneh, W., Owais, A., Nairoukh, M., 2013. An intelligent fuzzy based tracking controller for a dual-axis solar pv system. Automat. Construct. 29, 100–106.

Bedaouche, F., Gama, A., Hassam, A., Khelifi, R., Boubezoula, M., 2017. Fuzzy pid control of a dc motor to drive a heliostat. In: 2017 International Renewable and Sustainable Energy Conference (IRSEC). IEEE, pp. 1–6.

Berenguel, M., Rubio, F., Valverde, A., Lara, P., Arahal, M., Camacho, E., López, M., 2004. An artificial vision-based control system for automatic heliostat positioning offset correction in a central receiver solar power plant. Sol. Energy 76, 563–575.

Blanco-Muriel, M., Alarcón-Padilla, D.C., López-Moratalla, T., Lara-Coira, M., 2001. Computing the solar vector. Sol. Energy 70, 431–441.

Bosetti, V., Catenacci, M., Fiorese, G., Verdolini, E., 2012. The future prospect of pv and csp solar technologies: An expert elicitation survey. Energy Policy 49, 308–317.

Burhan, M., Oh, S.J., Chua, K.J.E., Ng, K.C., 2016. Double lens collimator solar feedback sensor and master slave configuration: Development of compact and low cost two axis solar tracking system for cpv applications. Sol. Energy 137, 352–363.

Camacho, E.F., Berenguel, M., 2012. Control of solar energy systems. IFAC Proc. Vol. 45, 848–855.

Carballo, J.A., Bonilla, J., Berenguel, M., Fernández-Reche, J., García, G., 2019. New approach for solar tracking systems based on computer vision, low cost hardware and deep learning. Renewable Energy 133, 1158–1166.

Carballo, J.A., Bonilla, J., Roca, L., Berenguel, M., 2018. New low-cost solar tracking system based on open source hardware for educational purposes. Sol. Energy 174, 826–836.

Casajús, L., Muñoz, I., 2016. Preliminary results after evaluating solar trackers based on iec 62817: 2014 ed. 1. In: AIP Conference Proceedings, AIP Publishing. p. 110001.

Chin, C., Babu, A., McBride, W., 2011. Design, modeling and testing of a standalone single axis active solar tracker using matlab/simulink. Renewable Energy 36, 3075–3090.

Chong, K.K., Wong, C.W., 2010. General formula for on-axis sun-tracking system. Sol. Collectors Panels, Theory Appl. 274–276.

Chong, K.K., Wong, C.W., Siaw, F.L., Yew, T.K., Ng, S.S., Liang, M.S., Lim, Y.S., Lau, S.L., 2009. Integration of an on-axis general sun-tracking formula in the algorithm of an open-loop sun-tracking system. Sensors 9, 7849–7865.

Chowdhury, M.E., Khandakar, A., Hossain, B., Abouhasera, R., 2019. A low-cost closed-loop solar tracking system based on the sun position algorithm. J. Sensors 2019.

Cristobal, A., Vega, A.M., López, A.L., 2012. Next Generation of Photovoltaics: New Concepts, vol. 165. Springer.

Debbache, M., Takilalte, A., Mahfoud, O., Karoua, H., Bouaichaoui, S., Laissaoui, M., Hamidat, A., 2016. Mathematical Model of an Azimuthal-elevation Tracking System of Small Scale Heliostat. International Science Press.

Del Rosario, A.J.R., Ubando, A.T., Culaba, A.B., 2019. Kinematic synthesis and analysis of a watt ii six-bar linkage for the design and validation of an open loop solar tracking mechanism. In: 2019 IEEE 11th International Conference on Humanoid, Nanotechnology, Information Technology, Communication and Control, Environment, and Management (HNICEM), IEEE. pp. 1–6.

Díaz, A., Keshtkar, S., Moreno, J.A., Hernandez, E., 2018. Design and control strategy of a low-cost parallel robot for precise solar tracking. In: International Conference on Robotics in Alpe-Adria Danube Region. Springer, pp. 342–350.

Domínguez, C., Antón, I., Sala, G., 2008. Solar simulator for concentrator photovoltaic systems. Opt. Express 16, 14894–14901.

El Kadmiri, Z., El Kadmiri, O., Masmoudi, L., Bargach, M.N., 2015. A novel solar tracker based on omnidirectional computer vision. J. Sol. Energy 2015.

El-Moghany, M.S., Hamed, B., 2012. Two axes sun tracker using fuzzy controller via pic16f877a. Two axes sun tracker using fuzzy controller via PIC16F877A.

El Shenawy, E., Kamal, M., Mohamad, M., 2012. Artificial intelligent control of solar tracking system. J. Appl. Sci. Res. 8, 3971–3984.

Elagib, S., Osman, N., 2013. Design and implementation of dual axis solar tracker based on solar maps. In: 2013 International Conference on Computing, Electrical and Electronic Engineering (ICCEEE). IEEE, pp. 697–699.

Engin, M., Engin, D., 2013. Optimization controller for mechatronic sun tracking system to improve performance. Adv. Mech. Eng. 5, 146352.

Fathabadi, H., 2016a. Comparative study between two novel sensorless and sensor based dual-axis solar trackers. Sol. Energy 138, 67–76.

Fathabadi, H., 2016b. Novel high efficient offline sensorless dual-axis solar tracker for using in photovoltaic systems and solar concentrators. Renewable Energy 95, 485–494.

Ferdaus, R.A., Mohammed, M.A., Rahman, S., Salehin, S., Mannan, M.A., 2014. Energy efficient hybrid dual axis solar tracking system. J. Renewable Energy 2014.

Fernandez-Prieto, J.A., Gadeo-Martos, M.A., Perez-Higueras, P., et al., 2020. Knowledge-based sensors for controlling a high-concentration photovoltaic tracker. Sensors 20, 1315.

Flores-Hernández, D., Palomino-Resendiz, S., Lozada-Castillo, N., Luviano-Juárez, A., Chairez, I., 2017. Mechatronic design and implementation of a two axes sun tracking photovoltaic system driven by a robotic sensor. Mechatronics 47, 148–159.

Garrido, R., Díaz, A., 2016. Cascade closed-loop control of solar trackers applied to hcpv systems. Renewable Energy 97, 689–696.

Ghassoul, M., 2018. Single axis automatic tracking system based on pilot scheme to control the solar panel to optimize solar energy extraction. Energy Reports 4, 520–527.

Hafez, A., Yousef, A., Harag, N., 2018. Solar tracking systems: Technologies and trackers drive types–a review. Renew. Sustain. Energy Rev. 91, 754–782. https://doi.org/10.1016/j.rser.2018.03.094.

Hamed, B., El-Moghany, M.S., 2012. Fuzzy controller design using fpga for sun tracking in solar array system. Fuzzy controller design using FPGA for sun tracking in solar array system 4.

Hammad, B.K., Fouad, R.H., Nijmeh, S.D., Mohsen, M., Tamimi, A., et al., 2014. Adaptive control of solar tracking system. IET Sci., Measur. Technol. 8, 426–431.

Hammoumi, A.E., Motahhir, S., Ghzizal, A.E., Chalh, A., Derouich, A., 2018. A simple and low-cost active dual-axis solar tracker. Energy Sci. Eng. 6, 607–620.

Hasanah, R.N., Setyawan, A.B., Maulana, E., Nurwati, T., Taufik, T., 2020. Computer-based solar tracking system for pv energy yield improvement. Int. J. Power Electron. Drive Syst. 11, 743.

Hoffmann, F.M., Molz, R.F., Kothe, J.V., Nara, E.O.B., Tedesco, L.P.C., 2018. Monthly profile analysis based on a two-axis solar tracker proposal for photovoltaic panels. Renewable Energy 115, 750–759.

Huang, B., Sun, F., 2007. Feasibility study of one axis three positions tracking solar pv with low concentration ratio reflector. Energy Convers. Manage. 48, 1273–1280.

Huang, C.H., Pan, H.Y., Lin, K.C., 2016. Development of intelligent fuzzy controller for a two-axis solar tracking system. Appl. Sci. 6, 130.

IEC, et al., 2014. IEC 62817: Photovoltaic Systems–Design qualification of solar trackers. International Electrotechnical Commission.

Ikhwan, M., Imron, C., et al., 2018. Model predictive control on dual axis solar tracker using matlab/simulink simulation. In: 2018 International Conference on Information and Communications Technology (ICOIACT). IEEE, pp. 784–788.

Jamroen, C., Komkum, P., Kohsri, S., Himananto, W., Panupintu, S., Unkat, S., 2020. A low-cost dual-axis solar tracking system based on digital logic design: Design and implementation. Sustainable Energy Technol. Assessm. 37, 100618.

Jianwattananukul, K., Locharoenrat, K., Lekchaum, S., 2016. Design and construction of new hybrid solar tracking system. In: Appl. Mech. Mater. Trans Tech Publ., pp. 510–515

Kang, H., Hong, T., Lee, M., 2019a. A new approach for developing a hybrid sun-tracking method of the intelligent photovoltaic blinds considering the weather condition using data mining technique. Energy Build. 109708.

Kang, H., Hong, T., Lee, M., 2019b. Technical performance analysis of the smart solar photovoltaic blinds based on the solar tracking methods considering the climate factors. Energy Build. 190, 34–48.

Keshtkar, S., 2017. High-order sliding mode control for solar tracker manipulator. In: Multibody Mechatronic Systems: Proceedings of the MUSME Conference Held in Florianópolis. Springer, p. 235.

Keshtkar, S., Keshtkar, J., Poznyak, A., 2016. Adaptive sliding mode control for solar tracker orientation. In: 2016 American Control Conference (ACC). IEEE, pp. 6543–6548.

Khalil, F.A., Asif, M., Anwar, S., ul Haq, S., Illahi, F., 2017. Solar tracking techniques and implementation in photovoltaic power plants: A review. Proc. Pakistan Acad. Sci. Phys. Comput. Sci. 54 (3), 231–241.

Khamooshi, M., Salati, H., Egelioglu, F., Hooshyar Faghiri, A., Tarabishi, J., Babadi, S., 2014. A review of solar photovoltaic concentrators. Int. J. Photoenergy 2014.

Kim, K.H., Cho, S.B., 2019. An efficient concentrative photovoltaic solar system with bayesian selection of optimal solar tracking algorithms. Appl. Soft Comput. 83, 105618.

Kivrak, S., 2013. Design of a low cost sun tracking controller system for photovoltaic panels. J. Renewable Sustainable Energy 5, 033119.

Kiyak, E., Gol, G., 2016. A comparison of fuzzy logic and pid controller for a single-axis solar tracking system. Renewables: Wind, Water, Sol. 3, 7.

Kost, C., Mayer, J.N., Thomsen, J., Hartmann, N., Senkpiel, C., Philipps, S., Nold, S., Lude, S., Saad, N., Schlegl, T., 2013. Levelized cost of electricity renewable energy technologies. In: Fraunhofer Institute for Solar Energy Systems ISE 144.

Kribus, A., Vishnevetsky, I., Yogev, A., Rubinov, T., 2004. Closed loop control of heliostats. Energy 29, 905–913.

Lee, C.Y., Chou, P.C., Chiang, C.M., Lin, C.F., 2009. Sun tracking systems: a review. Sensors 9, 3875–3890. https://doi.org/10.3390/s90503875.

Li, P.W., Kane, P., Mokler, M., 2013. Modeling of solar tracking for giant fresnel lens solar stoves. Sol. Energy 96, 263–273.
Limon, D., Alvarado, I., Alamo, T., Ruiz, M., Camacho, E.F., 2008. Robust control of the distributed solar collector field acurex using mpc for tracking. IFAC Proc. 41, 958–963.
Liu, G., Baba, A.O., Zhu, L., 2017. Hybrid controller for dual axes solar tracking system. In: 2017 36th Chinese Control Conference (CCC). IEEE, pp. 3203–3207.
Luque-Heredia, I., Gordillo, F., Rodriguez, F., 2004. A pi based hybrid sun tracking algorithm for photovoltaic concentration. In: Proceedings of the IEEE 19th European Photovoltaic Energy Conversion, pp. 7–14.
Luque-Heredia, I., Quéméré, G., Cervantes, R., Laurent, O., Chiappori, E., Chong, J.Y., 2012. The sun tracker in concentrator photovoltaics. In: Next Generation of Photovoltaics. Springer, pp. 61–93.
Mahmood, J.R., Muhammed, H., 2010. Design and implementation of smart relay based two-axis sun tracking system. In: 2010 1st International Conference on Energy, Power and Control (EPC-IQ). IEEE, pp. 259–263.
Makhija, S., Khatwani, A., Khan, M.F., Goel, V., Roja, M.M., 2017. Design & implementation of an automated dual-axis solar tracker with data-logging. In: 2017 International Conference on Inventive Systems and Control (ICISC). IEEE, pp. 1–4.
Mao, K., Liu, F., Ji, I.R., 2018. Design of arm-based solar tracking system. In: 2018 37th Chinese Control Conference (CCC), IEEE. pp. 7394–7398.
Mazumdar, D., Sinha, D., Panja, S., Dhak, D.K., 2015. Design of lqr controller for solar tracking system. In: 2015 IEEE International Conference on Electrical, Computer and Communication Technologies (ICECCT). IEEE, pp. 1–5.
Mi, Z., Chen, J., Chen, N., Bai, Y., Fu, R., Liu, H., 2016. Open-loop solar tracking strategy for high concentrating photovoltaic systems using variable tracking frequency. Energy Convers. Manage. 117, 142–149.
Mohammad, N., Karim, T., 2013. Design and implementation of hybrid automatic solar-tracking system. J. Sol. Energy Eng. 135.
Morón, C., Ferrández, D., Saiz, P., Vega, G., Díaz, J., 2017. New prototype of photovoltaic solar tracker based on arduino. Energies 10, 1298.
Motahhir, S., El Hammoumi, A., El Ghzizal, A., 2020. The most used mppt algorithms: Review and the suitable low-cost embedded board for each algorithm. J. Cleaner Product. 246, 118983.
Motahhir, S., Hammoumi, A.E., Ghzizal, A.E., Derouich, A., 2019. Open hardware/software test bench for solar tracker with virtual instrumentation. Sustainable Energy Technol. Assessm. 31, 9–16.
Mousazadeh, H., Keyhani, A., Javadi, A., Mobli, H., Abrinia, K., Sharifi, A., 2009. A review of principle and sun-tracking methods for maximizing solar systems output. Renewable Sustainable Energy Rev. 13, 1800–1818. https://doi.org/10.1016/j.rser.2009.01.022.
Mousazadeh, H., Keyhani, A., Javadi, A., Mobli, H., Abrinia, K., Sharifi, A., 2011. Design, construction and evaluation of a sun-tracking system on a mobile structure. J. Sol. Energy Eng. 133.
Murdock, H.E., Gibb, D., André, T., Appavou, F., Brown, A., Epp, B., Kondev, B., McCrone, A., Musolino, E., Ranalder, L., et al., 2019. Renewables 2019 global status report. REN 21- Reneawables Global Status Report.
Mustafa, G.E., Sidahmed, B.A., Nawari, M.O., 2019. The improvement of ldr based solar tracker's action using machine learning. In: 2019 IEEE Conference on Energy Conversion (CENCON). IEEE, pp. 230–235.
Nadia, A.R., Isa, N.A.M., Desa, M.K.M., 2018. Advances in solar photovoltaic tracking systems: A review. Renew. Sustain. Energy Rev. 82, 2548–2569.
Normanyo, E., Awingot, A.R., 2016. A solar radiation tracker for solar energy optimisation. Current J. Appl. Sci. Technol. 1–12.
Nsengiyumva, W., Chen, S.G., Hu, L., Chen, X., 2018. Recent advancements and challenges in solar tracking systems (sts): A review. Renew. Sustain. Energy Rev. 81, 250–279. https://doi.org/10.1016/j.rser.2017.06.085.
Okandeji, A., Olajide, M., Olasunkanmi, G., Jagun, Z., 2020. Analysis and implementation of a solar tracking rack system. Nigerian J. Technol. 39, 871–886.
Oladayo, B., Titus, A., 2016. Development of solar tracking system using imc-pid controller. Am. J. Eng. Res. 5, 135–142.
Ontiveros, J.J., Ávalos, C.D., Loza, F., Galán, N.D., Rubio, G.J., 2020. Evaluation and design of power controller of two-axis solar tracking by pid and fl for a photovoltaic module. Int. J. Photoenergy 2020.
Ozuna, G., Anaya, C., Figueroa, D., Pitalua, N., 2011. Solar tracker of two degrees of freedom for photovoltaic solar cell using fuzzy logic. In: Proceedings of the World Congress on Engineering, pp. 6–8.
Perers, B., Furbo, S., Dragsted, J., 2013. Thermal performance of concentrating tracking solar collectors. DTU R-292. Technical University of Denmark, DTU Byg.
Pérez-Higueras, P., Fernández, E.F., 2015. High Concentrator Photovoltaics: Fundamentals, Engineering and Power Plants. Springer.
Pérez-Higueras, P., Ferrer-Rodríguez, J.P., Almonacid, F., Fernández, E.F., 2018a. Efficiency and acceptance angle of high concentrator photovoltaic modules: Current status and indoor measurements. Renew. Sustain. Energy Rev. 94, 143–153.
Pérez-Higueras, P.J., Almonacid, F.M., Rodrigo, P.M., Fernández, E.F., 2018b. Optimum sizing of the inverter for maximizing the energy yield in state-of-the-art high-concentrator photovoltaic systems. Sol. Energy 171, 728–739.
Pişirir, O., Bingöl, O., 2016. Industrial pc based heliostat control for solar power towers. Acta Phys. Pol. A 130, 36–40.
Prinsloo, G., Dobson, R., 2015. Solar tracking. Stellenbosch: SolarBoo7s. ISBN 978Y0Y620Y61576Y1, 1–542.
Ranganathan, R., Mikhael, W., Kutkut, N., Batarseh, I., 2011. Adaptive sun tracking algorithm for incident energy maximization and efficiency improvement of pv panels. Renewable Energy 36, 2623–2626.
Reda, I., Andreas, A., 2004. Solar position algorithm for solar radiation applications. Sol. Energy 76, 577–589.
Rezoug, M.R., Chenni, R., 2018. The optimal angles of a dual-axis tracking system by pre-programmed method using a micocontroller. In: Int. J. Eng. Sci. Res. Technol..
Rhif, A., 2011. A position control review for a photovoltaic system: dual axis sun tracker. IETE Technical Rev. 28, 479–485.
Rhif, A., 2012. A sliding mode control for a sensorless tracker: application on a photovoltaic system. preprint arXiv:1204.1290.
Roos, T., Zwane, N., Perumal, S., Cathro, R., et al., 2008. A 25m 2 target-aligned heliostat with closed-loop control. In: Proceedings of ISES World Congress 2007 (Vol. I–Vol. V), Springer. pp. 1773–1781.
Roth, P., Georgiev, A., Boudinov, H., 2004. Design and construction of a system for sun-tracking. Renewable Energy 29, 393–402.
Rubio, F., Ortega, M., Gordillo, F., Lopez-Martinez, M., 2007. Application of new control strategy for sun tracking. Energy Convers. Manage. 48, 2174–2184.
Ruelas, J., Muñoz, F., Lucero, B., Palomares, J., 2019. Pv tracking design methodology based on an orientation efficiency chart. Appl. Sci. 9, 894.
Sabir, M.M., Ali, T., 2016. Optimal pid controller design through swarm intelligence algorithms for sun tracking system. Appl. Math. Comput. 274, 690–699.
Safan, Y.M., Shaaban, S., El-Sebah, M.I.A., 2017. Hybrid control of a solar tracking system using sui-pid controller. In: 2017 Sensors Networks Smart and Emerging Technologies (SENSET). IEEE, pp. 1–4.
Salgado-Conrado, L., 2018. A review on sun position sensors used in solar applications. Renew. Sustain. Energy Rev. 82, 2128–2146.
Sallaberry, F., Pujol-Nadal, R., Larcher, M., Rittmann-Frank, M.H., 2015. Direct tracking error characterization on a single-axis solar tracker. Energy Convers. Manage. 105, 1281–1290.
Sallaberry, F., Pujol-Nadal, R., Peres, B., 2017. Optical losses due to tracking on solar thermal collectors. Eurosun 2016, 1092–1103.
Satué, M.G., Castaño, F., Ortega, M.G., Rubio, F.R., 2020. Auto-calibration method for high concentration sun trackers. Sol. Energy 198, 311–323.
Sefa, I., Demirtas, M., Çolak, I., 2009. Application of one-axis sun tracking system. Energy Convers. Manage. 50, 2709–2718.
Seme, S., Štumberger, B., Hadžiselimović, M., 2016. A novel prediction algorithm for solar angles using second derivative of the energy for photovoltaic sun tracking purposes. Sol. Energy 137, 201–211.
Seme, S., Štumberger, G., 2011. A novel prediction algorithm for solar angles using solar radiation and differential evolution for dual-axis sun tracking purposes. Sol. Energy 85, 2757–2770.
Sidek, M., Azis, N., Hasan, W., Ab Kadir, M., Shafie, S., Radzi, M., 2017. Automated positioning dual-axis solar tracking system with precision elevation and azimuth angle control. Energy 124, 160–170.
Singh, R., Kumar, S., Gehlot, A., Pachauri, R., 2018. An imperative role of sun trackers in photovoltaic technology: A review. Renew. Sustain. Energy Rev. 82, 3263–3278.
Skouri, S., Ali, A.B.H., Bouadila, S., Salah, M.B., Nasrallah, S.B., 2016. Design and construction of sun tracking systems for solar parabolic concentrator displacement. Renew. Sustain. Energy Rev. 60, 1419–1429.
Sneineh, A.A., Salah, W.A., 2019. Design and implementation of an automatically aligned solar tracking system. Int. J. Power Electron. Drive Syst. 10, 2055.
Song, J., Yang, Y., Zhu, Y., Jin, Z., 2013. A high precision tracking system based on a hybrid strategy designed for concentrated sunlight transmission via fibers. Renewable Energy 57, 12–19.
Stamatescu, I., Făgărăşan, I., Stamatescu, G., Arghira, N., Iliescu, S.S., 2014. Design and implementation of a solar-tracking algorithm. Procedia Eng. 69, 500–507.
Su, Y., Zhang, Y., Shu, L., 2018. Experimental study of using phase change material cooling in a solar tracking concentrated photovoltaic-thermal system. Sol. Energy 159, 777–785.
Sumathi, V., Jayapragash, R., Bakshi, A., Akella, P.K., 2017. Solar tracking methods to maximize pv system output–a review of the methods adopted in recent decade. Renew. Sustain. Energy Rev. 74, 130–138. https://doi.org/10.1016/j.rser.2017.02.013.
Sungur, C., 2009. Multi-axes sun-tracking system with plc control for photovoltaic panels in turkey. Renewable Energy 34, 1119–1125.
Usta, M.A., Akyazi, Ö., Altaş, İ.H., 2011. Design and performance of solar tracking system with fuzzy logic controller used different membership functions. In: 2011 7th International Conference on Electrical and Electronics Engineering (ELECO). IEEE pp. II–381.
Victoria, M., Domínguez, C., Antón, I., Sala, G., 2009. Comparative analysis of different secondary optical elements for aspheric primary lenses. Opt. Express 17, 6487–6492.
Wang, J.M., Lu, C.L., 2013. Design and implementation of a sun tracker with a dual-axis single motor for an optical sensor-based photovoltaic system. Sensors 13, 3157–3168.
Wei, C.C., Song, Y.C., Chang, C.C., Lin, C.B., 2016. Design of a solar tracking system using the brightest region in the sky image sensor. Sensors 16, 1995.
Wiesenfarth, M., Philipps, S.P., Bett, A.W., Horowitz, K., Kurtz, S., 2017. Current status of concentrator photovoltaic (cpv) technology, 2017. Fraunhofer Institute for Solar Energy Systems ISE and National Renewable Energy Laboratory NREL: Washington, DC.
Xie, Q., Xiao, Y., Wang, X., Liu, D., Shen, Z., 2019. Heliostat cluster control for the solar tower power plant based on leader-follower strategy. IEEE Access 7, 135031–135039.
Yan, Z., Jiaxing, Z., 2010. Application of fuzzy logic control approach in a microcontroller-based sun tracking system. In: 2010 WASE International Conference on Information Engineering. IEEE, pp. 161–164.
Yang, C.K., Cheng, T.C., Cheng, C.H., Wang, C.C., Lee, C.C., 2017. Open-loop altitude-azimuth concentrated solar tracking system for solar-thermal applications. Sol. Energy 147, 52–60.

Yao, Y., Hu, Y., Gao, S., Yang, G., Du, J., 2014. A multipurpose dual-axis solar tracker with two tracking strategies. Renewable Energy 72, 88–98.
Yazidi, A., Betin, F., Notton, G., Capolino, G., 2006. Low cost two-axis solar tracker with high precision positioning. In: 2006 First International Symposium on Environment Identities and Mediterranean Area. IEEE, pp. 211–216.
Yeh, H.Y., Lee, C.D., 2012. The logic-based supervisor control for sun-tracking system of 1 mw hcpv demo plant: Study case. Appl. Sci. 2, 100–113.
Yilmaz, S., Ozcalik, H.R., Dogmus, O., Dincer, F., Akgol, O., Karaaslan, M., 2015. Design of two axes sun tracking controller with analytically solar radiation calculations. Renew. Sustain. Energy Rev. 43, 997–1005.
Zhang, J., Yin, Z., Jin, P., 2019. Error analysis and auto correction of hybrid solar tracking system using photo sensors and orientation algorithm. Energy.
Zhu, Y., Liu, J., Yang, X., 2020. Design and performance analysis of a solar tracking system with a novel single-axis tracking structure to maximize energy collection. Appl. Energy 264, 114647.